# SPECTRAL-COMPOSITIONAL VARIATIONS IN THE CONSTITUENT MINERALS OF MAFIC AND ULTRAMAFIC ASSEMBLAGES AND REMOTE SENSING IMPLICATIONS

EDWARD A. CLOUTIS

*Department of Geology, University of Alberta, Edmonton, Canada*

and

MICHAEL J. GAFFEY

*Department of Geology, West Hall, Rensselaer Polytechnic Institute, Troy, New York, U.S.A.*

(Received 3 December, 1990)

**Abstract.** The 0.3–2.6 $\mu$m reflectance spectra of most mafic and ultramafic assemblages can best be interpreted by considering the spectra as being composed of mafic silicate spectra modified by the presence of opaques, such as ilmenite or magnetite, and plagioclase feldspar. The systematic spectral-compositional relationships for olivine, orthopyroxene, and clinopyroxene have been examined and it has been determined that absorption band wavelength positions are correlated with ferrous iron content. Binary mafic silicate mixtures are generally less well understood, but certain spectral features such as reflectance maxima and minima wavelength positions and absorption band areas can be used to quantify or at least constrain end member abundances and compositions. The addition of opaques to a mafic silicate assemblage lowers overall reflectance and band depths. This differs from the effects of increasing grain size which are to lower overall reflectance but increase band depths. Plagioclase is relatively transparent compared to mafic silicates and must be present in appreciable amounts (tens of percent) to be spectrally detectable. The reflectance spectra of most mafic and ultramafic assemblages are dominated by mafic silicate absorption features and analysis of their spectra on this basis allows constraints to be placed on properties such as end member abundances and compositions.

## 1. Introduction

Basalts and other mafic (M) and ultramafic (UM) assemblages are important constituents of the surfaces of most bodies in the inner solar system. Basalts, their weathering products, or constituent minerals, are known or strongly inferred to exist on the surfaces of Mercury (McCord and Clark, 1979), Venus (Surkov *et al.*, 1983, 1986), the earth and moon (Basaltic Volcanism Study Project, 1981), Mars (Wood and Ashwal, 1981; Huguenin, 1987), and some asteroids and meteorites (Ma *et al.*, 1977; Gaffey, 1983). Spectroscopic remote sensing is one of the best means for characterizing M-UM assemblages on remote targets. These targets include extraterrestrial bodies and terrestrial occurrences which may not be amenable to widespread direct sampling for any number of reasons. Terrestrial occurrences are of additional importance because they can be associated with economically significant deposits of chromium, nickel, and platinum group elements (Hunt and Wynn, 1979; Evans, 1980; King and Ridley, 1987).

*Earth, Moon, and Planets* **53**: 11–53, 1991.

The principal minerals comprising the M-UM rocks considered here are orthopyroxene (OPX), clinopyroxene (CPX), olivine (OLV), plagioclase feldspar (PLG), and the opaque minerals magnetite (MAG) and ilmenite (ILM). The ultraviolet, visible, and near-infrared spectral reflectance properties of these minerals and their various combinations have been examined by previous investigators and as part of this study. Spectral reflectance studies are particularly useful because the data available from laboratory studies can be directly compared to that acquired by remote sensing means. Each mineral exhibits certain unique spectral characteristics which aid in its identification using reflectance spectroscopy. Reflectance spectra of two or more minerals are not simple weighted averages of the end member spectra but exhibit complex spectra dependent on a number of factors. Theoretical, semi-empirical, and empirical methods have been developed to deal with the non-linearity of mixture spectra (e.g. Hapke, 1981; Johnson *et al.*, 1983; Cloutis *et al.*, 1986; Crown and Pieters, 1987; Sunshine *et al.*, 1990). The reflectance spectra of single phases, two-, three-, and four-component mixtures have been examined in the laboratory and combined with the results of previous investigations in order to better understand the most important factors which affect the reflectance spectra of M-UM assemblages. The spectra of M-UM rocks are then examined in light of these results in order to determine whether mineral mixtures are useful spectral analogues for them.

Basalts, which are the major focus of this study, can be thought of as mixtures of three spectral types of materials: strongly featured minerals (pyroxene, olivine), weakly featured, relatively transparent minerals (plagioclase), and strongly absorbing, neutral minerals (magnetite, ilmenite). Using this analogy, the reflectance spectra of mafic silicate-bearing rocks will be dominated by the mafic silicates and modified by the other phases; i.e. mafic silicate absorption bands will be persistent but modified. Thus, the strategy adopted here is to examine how mafic silicate spectra are modified by the presence of other mafic silicates and the additional phases. Spectral data are examined for progressively more complex mixtures (containing two, three and four components).

## 2. Experimental Procedure

The compositions of the various minerals used in this study have been determined by electron microprobe analysis at the University of Calgary SEMQ facility and are averages of 4–8 point analyses and area scans. The data have been reduced using Bence-Albee $\alpha$ and $\beta$ correction factors. Ferrous iron values have been obtained by wet chemical methods and ferric iron as the difference between total and ferrous iron. The chemical analyses of some of the minerals used in this study are given in Table I.

The reflectance spectra of powdered samples have been measured in all cases. The powders were prepared by crushing the samples in an alumina mortar and pestle. Any impurities were removed through a combination of magnetic separ-

TABLE I

Chemical analyses of some of the samples used in this study

| Wt. % | ILM101 | MAG101 | OLV003 | PLG108 | PY003 | PYX009 |
|---|---|---|---|---|---|---|
| $SiO_2$ | 0.20 | 0.00 | 40.64 | 46.55 | 50.33 | 53.90 |
| $Al_2O_3$ | 0.01 | 0.33 | tr. | 32.70 | 5.46 | 0.51 |
| FeO | 45.43 | 26.52 | 9.25 | N.D. | 17.30 | 6.20 |
| $Fe_2O_3$ | N.D. | 63.71 | 0.59 | 0.64[1] | 1.43 | 0.00 |
| MgO | 0.01 | 3.63 | 49.13 | 0.04 | 23.58 | 14.18 |
| CaO | N.D. | N.D. | 0.07 | 17.28 | 1.59 | 25.08 |
| $Na_2O$ | N.D. | N.D. | 0.00 | 1.71 | 0.05 | 0.05 |
| $TiO_2$ | 47.61 | 3.04 | 0.00 | 0.05 | 0.41 | 0.01 |
| $Cr_2O_3$ | 0.02 | 0.03 | 0.01 | 0.03 | 0.11 | 0.04 |
| $V_2O_5$ | N.D. | N.D. | 0.00 | 0.01 | 0.02 | 0.02 |
| CoO | N.D. | N.D. | 0.04 | 0.03 | 0.04 | 0.05 |
| NiO | N.D. | N.D. | 0.33 | 0.09 | 0.01 | 0.15 |
| MnO | 0.02 | 0.60 | 0.09 | 0.01 | 0.29 | 0.26 |
| ZnO | N.D. | N.D. | 0.00 | 0.02 | N.D. | N.D. |
| $K_2O$ | N.D. | N.D. | N.D. | 0.02 | N.D. | N.D. |
| SrO | N.D. | N.D. | N.D. | 0.03 | N.D. | N.D. |
| BaO | N.D. | N.D. | N.D. | 0.03 | N.D. | N.D. |
| Total | 93.30 | 97.86 | 100.15 | 99.24 | 100.62 | 100.45 |
| | | | Atomic ratios | | | |
| Mg | – | – | 90.4 | – | 68.5 | 39.8 |
| $Fe^{2+}$ | – | – | 9.6 | – | 28.2 | 9.7 |
| Ca | – | – | – | – | 3.3 | 50.5 |

| Wt.% | PYX018 | PYX020 | PYX032 | PYX036 | PYX040 | PYX042 | PYX117 |
|---|---|---|---|---|---|---|---|
| $SiO_2$ | 55.17 | 55.23 | 50.21 | 50.54 | 47.27 | 56.59 | 53.54 |
| $Al_2O_3$ | 0.37 | 0.59 | 1.24 | 2.99 | 8.28 | 0.09 | 1.54 |
| FeO | 2.42 | 2.07 | 23.65 | 8.18 | 4.69 | 8.93 | 16.17 |
| $Fe_2O_2$ | 0.00 | 0.00 | 5.11 | 1.71 | 2.77 | 0.84 | 1.02 |
| MgO | 17.01 | 17.06 | 17.57 | 14.64 | 13.19 | 33.88 | 27.53 |
| CaO | 23.93 | 24.08 | 1.59 | 20.35 | 20.90 | 0.22 | 0.35 |
| $Na_2O$ | 0.51 | 0.52 | 0.00 | 0.27 | 0.63 | 0.00 | 0.00 |
| $TiO_2$ | tr. | 0.09 | 0.19 | 0.86 | 1.73 | 0.04 | 0.03 |
| $Cr_2O_3$ | 0.91 | 0.96 | 0.04 | 0.07 | 0.43 | 0.04 | 0.07 |
| $V_2O_5$ | 0.03 | 0.05 | tr. | 0.08 | tr. | tr. | 0.00 |
| CoO | 0.02 | 0.05 | 0.06 | 0.04 | 0.03 | 0.02 | 0.01 |
| NiO | 0.07 | 0.06 | 0.01 | 0.02 | 0.03 | 0.01 | 0.05 |
| MnO | 0.10 | 0.10 | 0.53 | 0.25 | 0.11 | 0.04 | 0.44 |
| ZnO | N.D. | N.D. | N.D. | N.D. | N.D. | N.D. | N.D. |
| $K_2O$ | N.D. | N.D. | N.D. | N.D. | N.D. | N.D. | N.D. |
| SrO | N.D. | N.D. | N.D. | N.D. | N.D. | N.D. | N.D. |
| BaO | N.D. | N.D. | N.D. | N.D. | N.D. | N.D. | N.D. |
| Total | 100.54 | 100.86 | 100.20 | 100.00 | 100.06 | 100.70 | 100.75 |
| | | | Atomic ratios | | | | |
| Mg | 47.8 | 48.0 | 54.9 | 43.3 | 42.7 | 86.8 | 74.7 |
| $Fe^{2+}$ | 3.8 | 3.3 | 41.5 | 13.4 | 8.5 | 12.8 | 24.6 |
| Ca | 48.4 | 48.7 | 3.6 | 43.3 | 48.8 | 0.4 | 0.7 |

[1] All Fe reported as $Fe_2O_3$. tr. = <0.01 wt %. N.D. = not determined.

ation and hand-picking. The cleaned samples were repeatedly wet sieved with acetone to obtain well-sorted size ranges.

The reflectance spectra have been variously acquired using spectrometer facilities located at the University of Hawaii (UH), the NASA RELAB instrument at Brown University in Providence, Rhode Island (RELAB), or the U.S. Geological Survey instrument in Boulder, Colorado (USGS). The UH spectra have been measured in bidirectional reflectance mode ($i = 0°$, $e = 15°$), the RELAB spectra in bidirectional reflectance mode ($i = 0°$, $e = 15°$ and/or $i = 30°$, $e = 0°$), while the USGS spectra have been measured using an integrating sphere. Details of the various instruments are given by Singer (1981 – UH), Pieters (1983 – RELAB), and King and Ridley (1987 – USGS). All spectra have been measured relative to halon, a near-perfect diffuse reflector in the 0.3- to 2.6-$\mu$m region (Weidner and Hsia, 1981), and corrected for minor (~2%) irregularities in halon's absolute reflectance in the 2 $\mu$m region, as well as for dark current offsets. The reflectance spectra were processed using either SPECPR (Clark, 1980) or its PC-compatible version, the Gaffey Spectrum Processing System.

Continuum removal has been performed in some cases in order to isolate specific absorption bands. This was accomplished by dividing out a straight line continuum tangent to the reflectance spectrum on either side of the absorption band. Band centers and band minima were calculated by fitting a quadratic equation to ~10–20 data points on either side of a visually determined center or minimum. Band depths ($D_b$) have been calculated using Equation (32) of Clark and Roush (1984).

A number of spectral parameters have been found to be useful for extracting compositional information from mafic silicate-bearing mixture spectra (Cloutis *et al.*, 1986), some of which are shown in Figure 1. These include the local reflectance maximum in the 0.5–0.8 $\mu$m spectral region (0.7 $\mu$m peak), the major absorption bands located in the 1 $\mu$m region (band I) and 2 $\mu$m region (band II), and the local reflectance maximum between band I and band II (interband peak). The areas of absorption bands are also useful for spectral deconvolution. The band II* area is the region enclosed by a horizontal line tangent to the spectrum at the interband peak, a vertical line positioned at the band II minimum, and the spectrum itself (Figure 1). The vertical line is used because the long wavelength wing of band II is often at lower reflectance than the interband peak and consequently a horizontal line would often fail to intersect the spectrum at longer wavelengths. The band I area is the region enclosed by the spectrum and a straight line continuum tangent to the spectrum at the 0.7 $\mu$m peak and the interband peak (Figure 1). The band I* area is this area multiplied by the reflectance ratio of the interband peak to the 0.7 $\mu$m peak. This reflectance ratio is used to compensate for any difference in reflectance between the two peaks which may tend to alter the band I area. In all cases, the band II*/I* area ratio is used because it yields a dimensionless number, removing the dependence of the areas on the particular spectral scale used. The tangent intercept (Figure 1) is the wavelength position where a horizontal line, tangent to the spectrum at the 0.7 $\mu$m peak, intersects the long wavelength wing of band I.

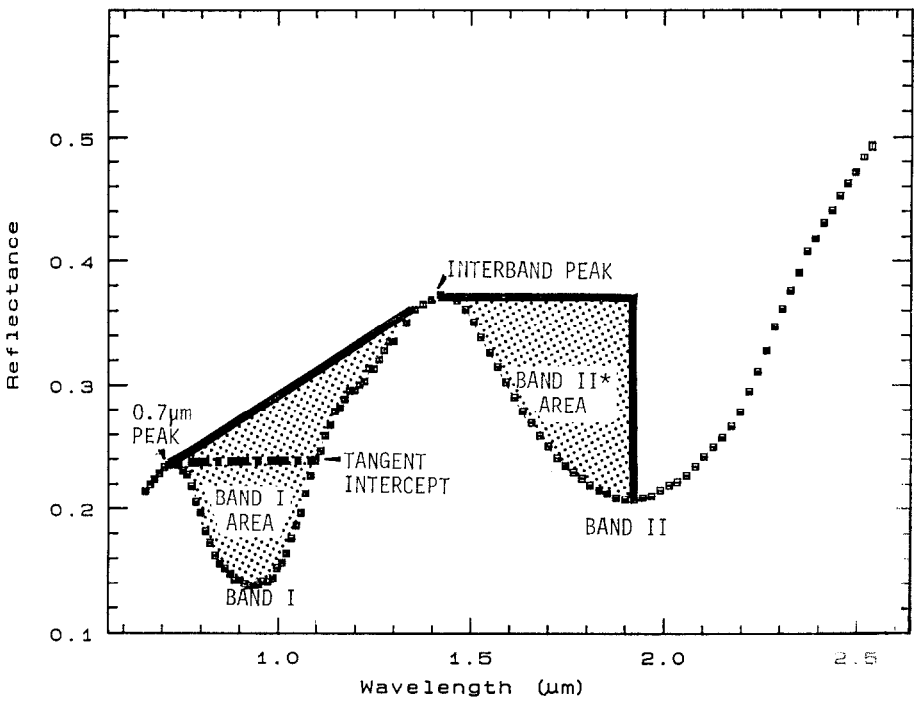


Fig. 1. Reflectance spectrum of a 50/50 mixture of 45–90 $\mu$m sized orthopyroxene (PYX003) and olivine (OLV003) illustrating a number of spectral parameters (spectrum measured at UH). Band area I* = (band area I/(interband peak/0.7 $\mu$m peak)).

## 3. Pure Phase Spectra

The 0.3–2.6 $\mu$m reflectance spectra of the most important M-UM constituent minerals (OPX, CPX, OLV, PLG, MAG, ILM) have been examined in order to determine the quality and quantity of compositional information amenable to spectral determination. The most important characteristic of a single phase is, of course, composition. For mineral mixtures, both composition and end member abundances are important. Knowledge of end member abundances and compositions are essential for deducing the geological history of a particular M-UM assemblage. The reflectance spectra of pure phases are dealt with first followed by increasingly complex mixtures. Finally the reflectance spectra of various naturally occurring M-UM assemblages are examined in light of these results.

### 3.1. Pyroxene

Pyroxene is a major component of many mafic and ultramafic rock types such as basalts, gabbros, norites, pyroxenites, peridotites, and diabases. Of the minerals considered in this study, pyroxenes have been the subject of the most spectral studies (e.g. Bancroft and Burns, 1967; Burns *et al.*, 1972; Pieters, 1974; Adams, 1974, 1975; Hazen *et al.*, 1978; Cloutis, 1985). Pyroxenes are broadly divided into two main subtypes on the basis of calcium content – orthopyroxenes (low Ca) and

clinopyroxenes (high Ca). A large number of pyroxene spectra have been measured for this study to complement the existing data.

Orthopyroxene reflectance spectra are characterized by the two major absorption bands situated near 1 $\mu$m (band I) and 2 $\mu$m (band II) (Figure 2). Both bands are attributable to crystal field transitions in ferrous iron located in the M2 crystallographic site. There are also a number of weaker absorption bands present in the ultraviolet and visible regions and a reflectance decrease shortward of $\sim$0.5 $\mu$m attributable to various charge transfers and crystal field transitions (Clark, 1957; White and Keester, 1966; Burns, 1970b; Burns *et al.*, 1972; Roush, 1984).

Both band I and band II shift to longer wavelengths with increasing ferrous iron content (Adams, 1974; Cloutis, 1985; Aoyama *et al.*, 1987). The band I minimum varies between $\sim$0.9 $\mu$m and 0.94 $\mu$m and band II between $\sim$1.8 $\mu$m and 2.1 $\mu$m. The existing transmittance and reflectance spectral data for band minimum wavelength position have been combined with the data from this study in order to identify the spectral-compositional trends. However, there appears to be a systematic offset between the data of Adams (1974, 1975) and other investigators (McFadden *et al.*, 1982). Analysis of this offset suggests that it is on the order of 13 nm; i.e. the Adams data are, on average, shifted towards shorter wavelengths by this amount. Until the Adams samples are recharacterized, or the cause of this offset determined, a 13 nm offset correction has been applied to his data in order to be able to extract useful information from it. The variation in band I and band II orthopyroxene minima appears to be systematic – both bands shift to longer wavelengths with increasing iron content (Figure 3). These trends can also be projected onto the pyroxene tetralateral (Figure 4) so that determination of orthopyroxene band positions provides a rapid means for constraining orthopyroxene major element contents.

Changes in mean grain size also affect spectral reflectance. Increasing particle size results in a decrease in overall reflectance and an increase in absorption band depths up to a point at which the absorption bands become saturated (Hunt and Salisbury, 1970; Adams and Filice, 1967; Pieters, 1974). This relationship for various orthopyroxenes is shown in Figure 5.

Clinopyroxene spectra can be divided into two types on the basis of absorption band positions and shapes, and are designated type A and type B. Type B spectra are superficially similar to orthopyroxenes, exhibiting two major absorption bands near 1.05 $\mu$m and 2.3 $\mu$m (Figure 2). These bands are attributable to crystal field transitions in ferrous iron situated in the M2 crystallographic site. Type A spectra exhibit two major, partially overlapping absorption bands near 0.9 and 1.15 $\mu$m due to crystal field transitions in ferrous iron located in the M1 crystallographic site (Figure 2). Intermediate type A-B clinopyroxene spectra are also known and are due to contributions by ferrous iron in both the M1 and M2 sites. Many clinopyroxenes display an additional absorption band near 0.8 $\mu$m due to $Fe^{2+}$–$Fe^{3+}$ charge transfers. Minor absorption bands attributable to various charge

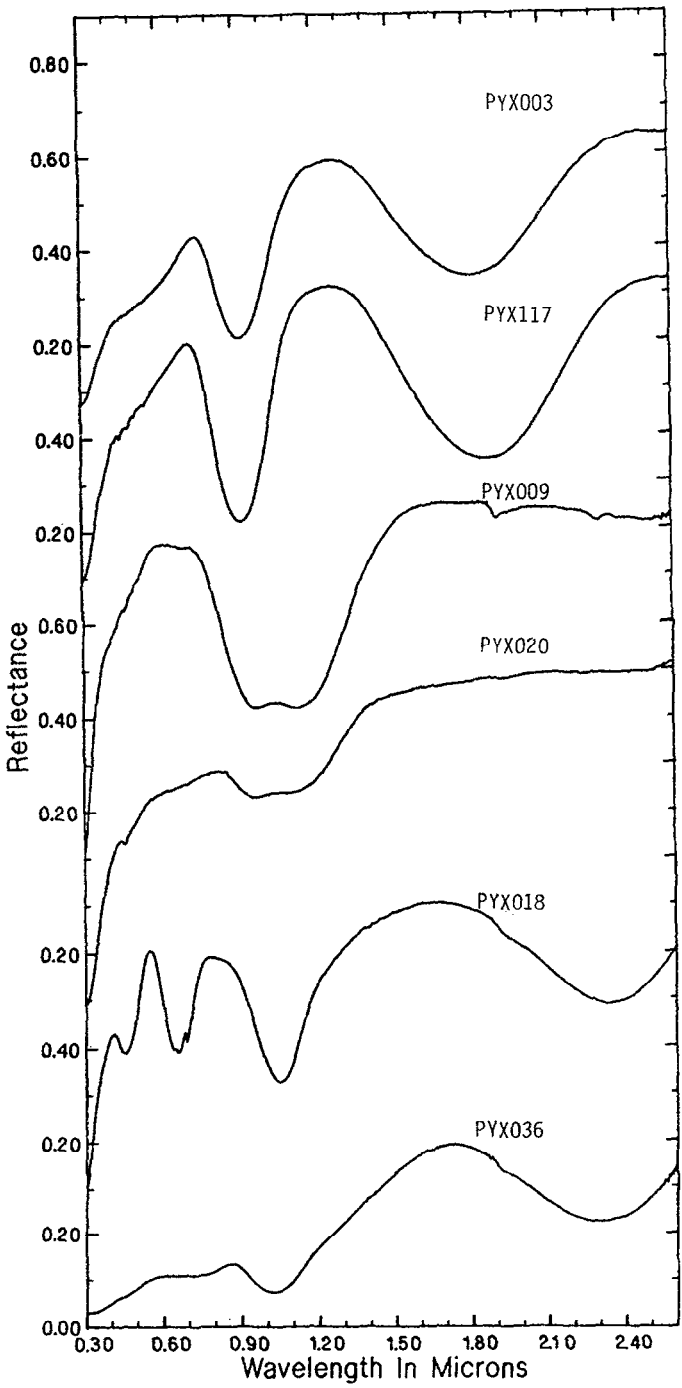


Fig. 2. Reflectance spectra (0.3–2.6 $\mu$m) of orthopyroxenes (PYX003, PYX117, <45 $\mu$m grain size) spectral type A clinopyroxenes (PYX009 –45–90 $\mu$m grain size, PYX020 <45 $\mu$m grain size), and spectral type B clinopyroxenes (PYX018, PYX036, 45–90 $\mu$m grain size. Spectra measured at RELAB ($i = 30°$, $e = 0°$). Chemical analyses are given in Table I.

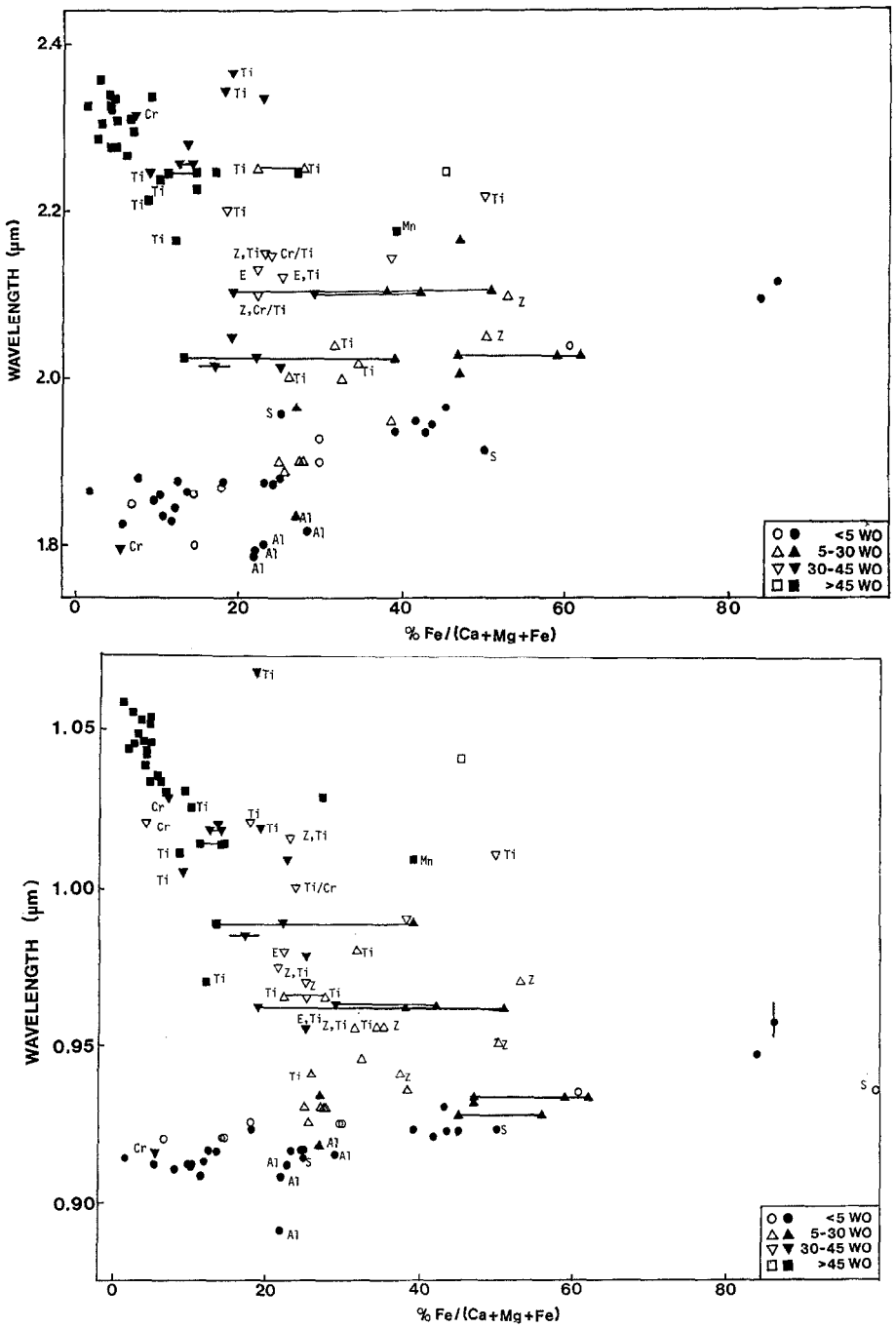


Fig. 3. Band I (lower) and band II (upper) minima wavelength positions for pyroxenes as a function of ferrosilite (Fs) content. Open symbols indicate transmission spectra (Hazen *et al.*, 1978), filled symbols indicate reflectance spectra (this study, Adams, 1974,1975). The various samples have been subdivided into four groups on the basis of wollastonite (Wo) content. Ti = samples containing >1 wt% $TiO_2$, Cr = samples containing >1 wt% $Cr_2O_3$, Mn = samples containing >5 wt% Mn, E = samples known to contain exsolved phases, Z = strongly zoned samples, Al = orthopyroxenes containing >4 wt% $Al_2O_3$, S = synthetic samples.

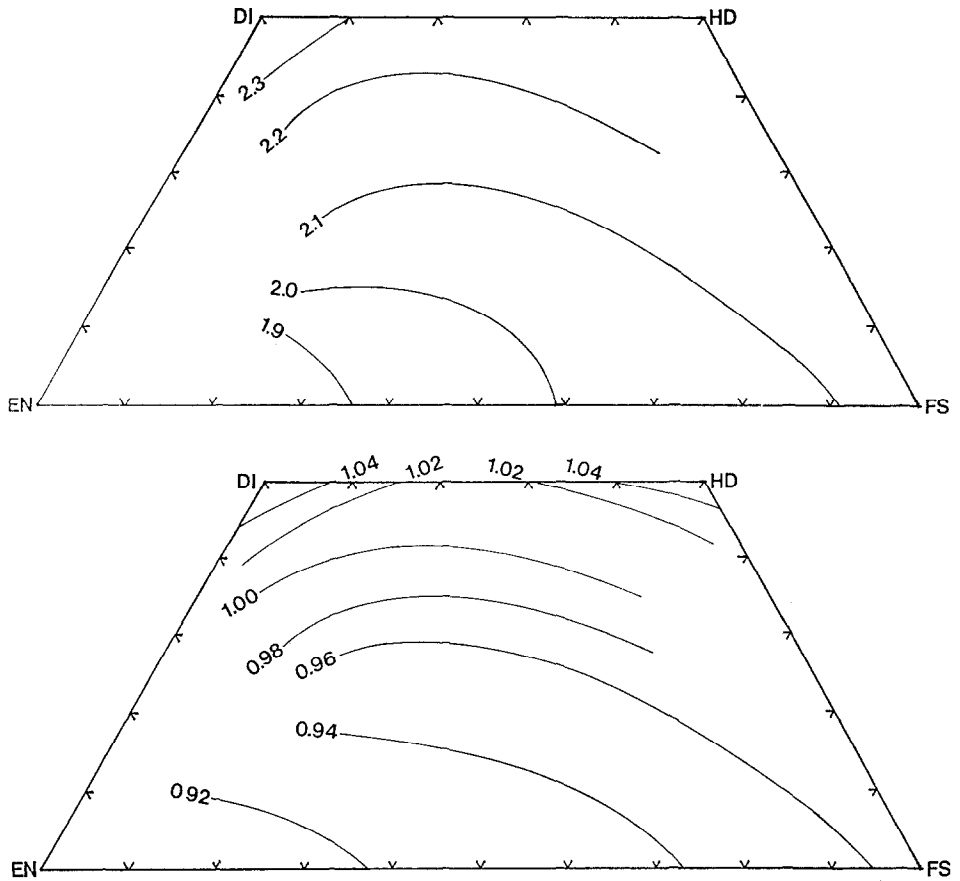


Fig. 4. Pyroxene band I (lower) and band II (upper) minima wavelength positions projected onto the pyroxene tetralateral and contoured. Contours have been terminated where no sample spectra are available. Sources of data: Adams (1974, 1975), Hazen *et al.* (1978), this study.

transfers and crystal field transitions are often superimposed on the intense charge transfer-related reflectance decrease shortward of ~0.5 $\mu$m (Burns, 1970b; Burns *et al.*, 1972; Adams and McCord, 1972; Adams, 1974, 1975; Hazen *et al.*, 1978; Rossman, 1980).

The compilation of existing and new spectral data for clinopyroxenes indicates that certain systematic spectral-compositional trends exist. The wavelength positions of the two major $Fe^{2+}$ absorption bands of type B clinopyroxenes do not show a simple linear relationship with $Fe^{2+}$ and Ca abundances (Figure 3). It appears that with increasing iron content, the correlation changes from positive to negative. Spectral-compositional relationships are further obscured because clinopyroxenes frequently contain appreciable quantities of other cations and compositional inhomogeneities in the form of exsolution features and pronounced zonations (Huebner, 1980; Rossman, 1980), and by the lack of spectral data for large regions of the pyroxene tetralateral. Nevertheless, certain trends have been

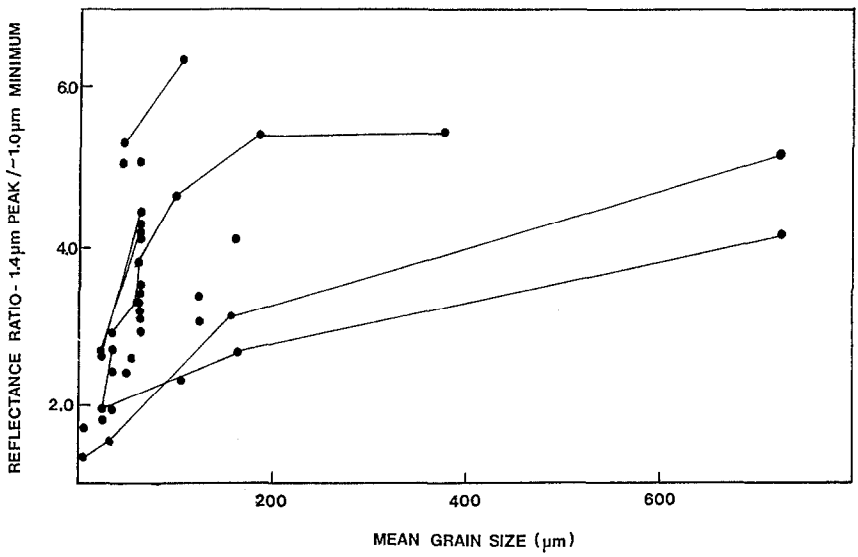


Fig. 5. Reflectance ratio of the interband peak near 1.4 $\mu$m to the band I minimum near 1 $\mu$m, as a function of mean grain size for orthopyroxenes. Lines connect different grain sizes of a single mineral. Sources of data: Hunt and Salisbury (1970), Adams, (1974), Pieters (1983), this study.

tentatively identified, allowing absorption band minimum wavelength position contours to be constructed on the pyroxene compositional tetralateral (Figure 4).

Spectral type A clinopyroxene data are much less abundant than type B spectral data. There exists a general, but by no means inviolable, compositional separation between the two spectral types. Type A samples generally contain >50 mol% Wo while type B samples generally contain <50 mol% Wo (Figure 6). The vast majority of clinopyroxenes found in basaltic and most other M-UM assemblages contain <50% Wo (Robinson, 1980), so that focusing on spectral type B clinopyroxenes is justified. No systematic spectral-compositional trends have been found for type A specimens due to the small number of samples (10), and because of the common presence of a broad, intense wavelength decrease toward shorter wavelengths which tends to obscure the $Fe^{2+}$ absorption bands. As with orthopyroxenes, clinopyroxene band depths increase with increasing particle size (Hunt and Salisbury, 1970; Cloutis, 1985).

### 3.2. Olivine

The reflectance spectra of olivines are dominated by a broad absorption feature centered near 1.05 $\mu$m which is composed of three partially overlapping absorption bands (Figure 7). The strong central band is due to crystal field transitions in ferrous iron located in the M2 site. The weaker bands on either side are assigned to similar transitions in ferrous iron located in the M1 site (White and Keester, 1966; Burns, 1970a; Burns, 1974; Runciman *et al.*, 1974). Olivine spectra also display minor absorption bands in the ultraviolet and visible regions due to various

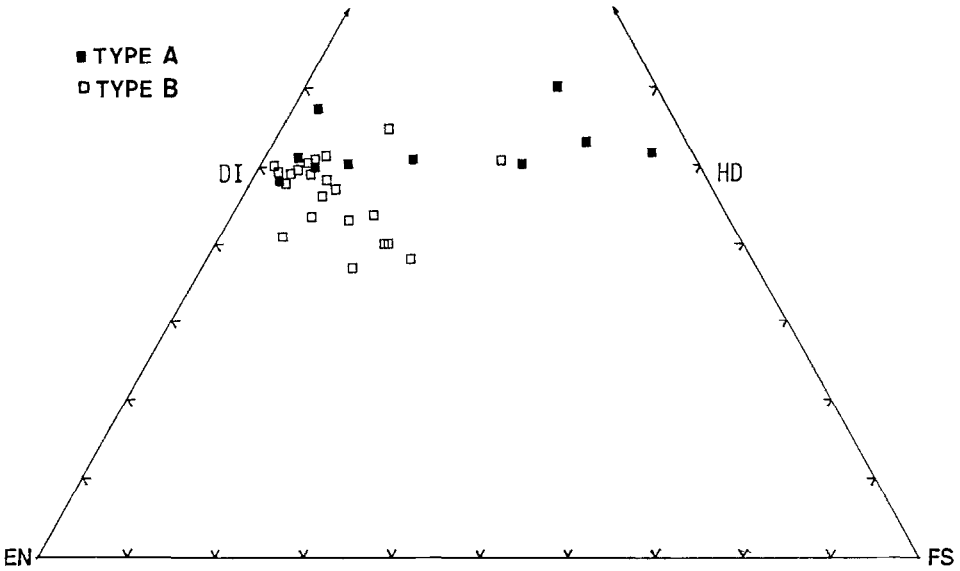


Fig. 6. Clinopyroxene compositions projected onto the pyroxene tetralateral illustrating the partial separation between spectral types A and B on the basis of calcium content.

crystal field transitions and charge transfers. These are frequently superimposed on the steep reflectance dropoff shortward of ~0.5 $\mu$m due to various charge transfers (Cloutis, 1985 and references given therein; King and Ridley, 1987).

It has been known for some time that the major absorption bands move to longer wavelengths with increasing iron content (Burns, 1970a; Burns *et al.*, 1972). A compilation of existing high-quality spectra of natural olivines for which compositional information exists (Miyamoto *et al.*, 1981; Singer, 1981; Cloutis, 1985; King and Ridley, 1987) and the results of this study illustrate this relationship (Figure 8). There is some scatter in the data, some due to unknown causes but some the result of contamination by other phases. As with pyroxenes, the depth of band I increases with increasing grain size until the band becomes saturated at a reflectance ratio of ~10 (Figure 9).

### 3.3. Plagioclase feldspar

Plagioclase feldspars, primarily because they contain only small amounts of transition series elements, primarily iron, exhibit weakly featured reflectance spectra of high overall reflectance. Their spectra show a single, broad, weak absorption band centered near 1.25 $\mu$m due to crystal field transitions in ferrous iron (Figure 7). The wavelength position of this band is dependent on the anorthite content which in turn is related to the iron content (Adams, 1975; Adams and Goullaud, 1978). As expected, band depth increases with increasing iron content and overall reflectance decreases with increasing grain size (Hunt and Salisbury, 1970; Hunt *et al.*, 1973; Adams, 1975; Adams and Goullaud, 1978). Few additional feldspars were spectrally characterized for this study because the spectral-compositional

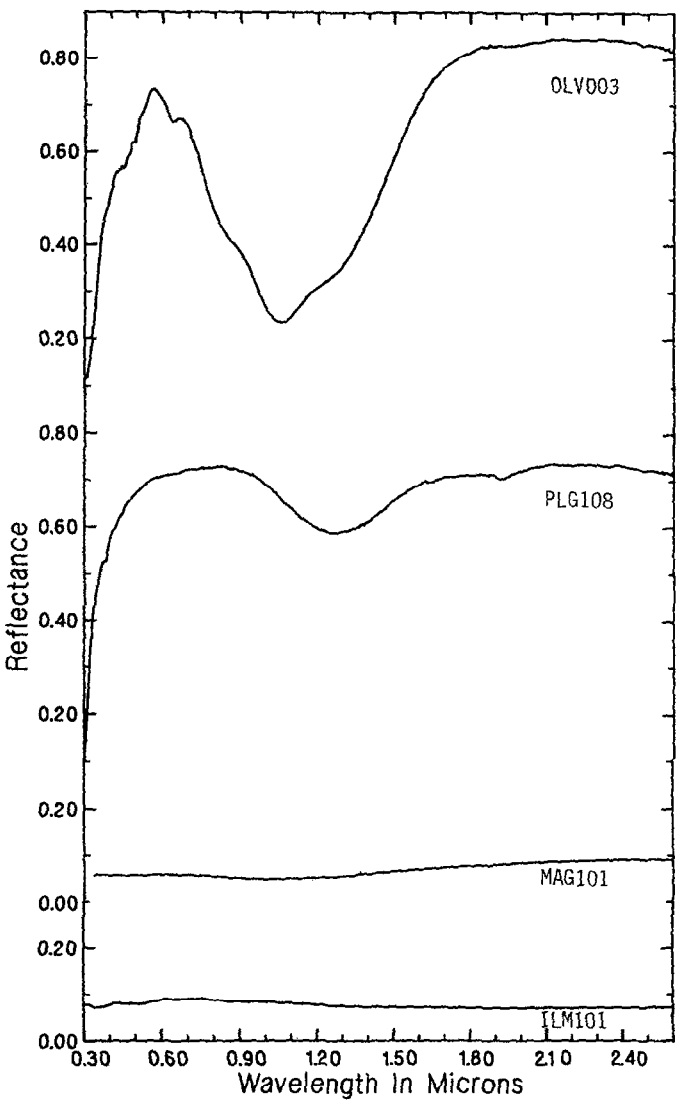


Fig. 7. Reflectance spectra (0.3–2.6 $\mu$m) of 45–90 $\mu$m size samples of olivine (OLV003), plagioclase (PLG108), magnetite (MAG101), and ilmenite (ILM101). Spectra measured at RELAB ($i = 0°$, $e = 15°$ for OLV, MAG; $i = 30°$, $e = 0°$ for PLG, ILM).

relationships are well established and because plagioclase is such a weak absorber relative to the mafic silicates (Adams, 1974; Nash and Conel, 1974; Morris, 1985; Crown and Pieters, 1987).

### 3.4. Opaque minerals

Magnetite and ilmenite are the major opaque phases present in terrestrial and lunar M-UM assemblages, respectively (Smith and Steele, 1976; Basaltic Volcanism Study Project, 1981). The reflectance spectrum of magnetite exhibits very low

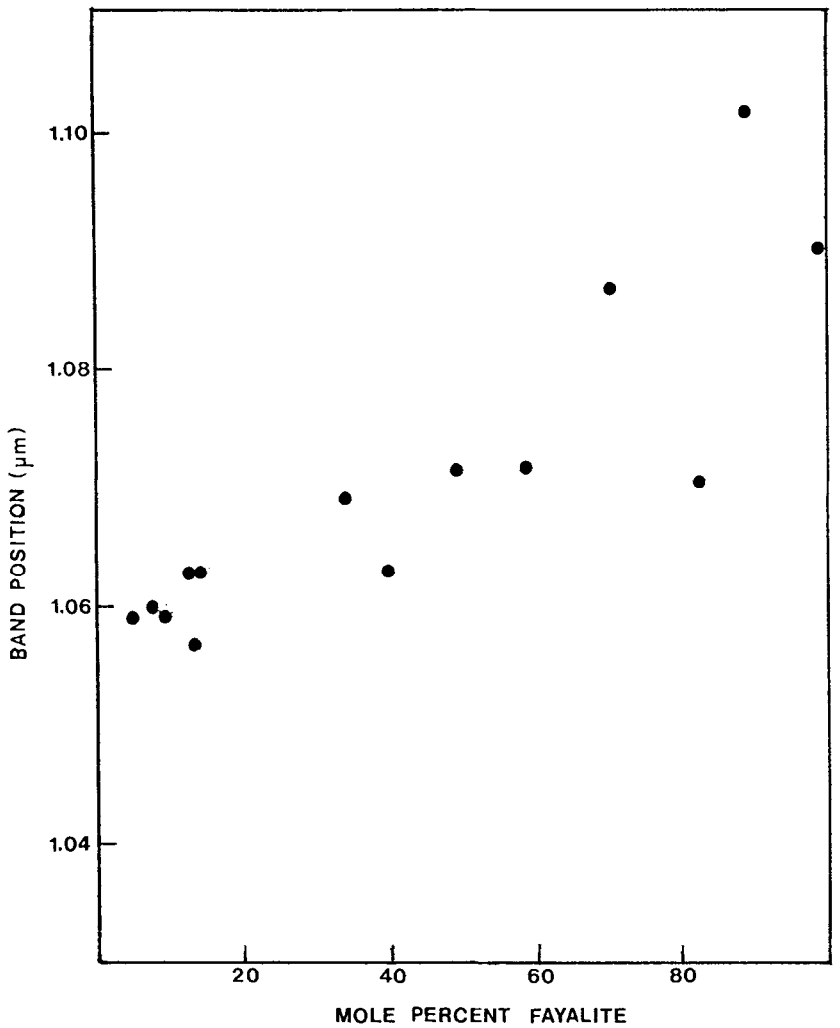


Fig. 8. Wavelength position of olivine band I centers (after division of a straight line continuum) as a function of ferrous iron content. Sources of data: This study, King and Ridley (1987).

overall reflectance, a reflectance maximum near 0.8 $\mu$m, and either a weak $Fe^{2+}$ absorption band near 1 $\mu$m or a reflectance decline longward of 0.8 $\mu$m (Hunt *et al.*, 1971; Adams, 1975; Gradie and Veverka, 1980; Singer, 1981; Morris *et al.*, 1985; Wagner *et al.*, 1987; Cloutis *et al.*, 1990c). Compared to mafic silicate and feldspar spectra, magnetite is essentially featureless, flat and opaque (Figure 7). Its overall reflectance decreases with decreasing particle size.

Ilmenite spectra exhibit a broad iron-titanium charge transfer absorption band near 0.5 $\mu$m, and a broad, weak $Fe^{2+}$ absorption feature between 1.2 $\mu$m and 1.5 $\mu$m (Figure 7; Hunt *et al.*, 1971; Nash and Conel, 1974; Adams, 1974, 1975; Pieters, 1983; Cloutis *et al.*, 1990d). Again, overall reflectance decreases with

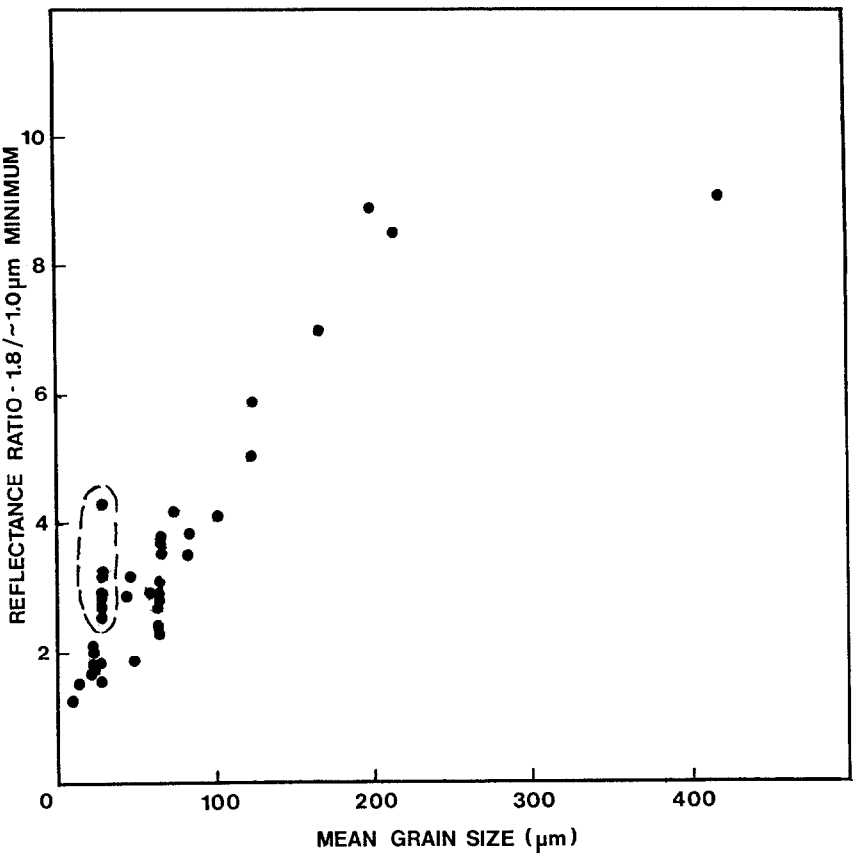


Fig. 9. Ratio of the absolute reflectance at 1.8 $\mu$m to the reflectance of the band I minimum near 1 $\mu$m, as a function of mean grain size. The points enclosed by the dashed line are some iron-rich olivines which deviate from the general trend. Sources of data: this study, King and Ridley (1987).

decreasing particle size (Hunt *et al.*, 1971). The various absorption bands only become apparent when reflectance scales are greatly reduced.

## 4. Two Phase Mixture Spectra

The most important two-phase mixtures for the purposes of interpreting M-UM reflectance spectra are those involving two mafic silicates – OPX + OLV, OPX + CPX, and CPX + OLV. The most important parameters it is hoped to derive from spectral analysis of such mixtures are end member abundances and compositions.

### 4.1. Orthopyroxene + olivine spectra

The spectral systematics of OPX + OLV mixtures have been examined previously by Adams (1974), Singer (1981), Miyamoto *et al.* (1983), Johnson *et al.* (1983), Cloutis (1985) and Cloutis *et al.* (1986). Semi-quantitative studies are also found

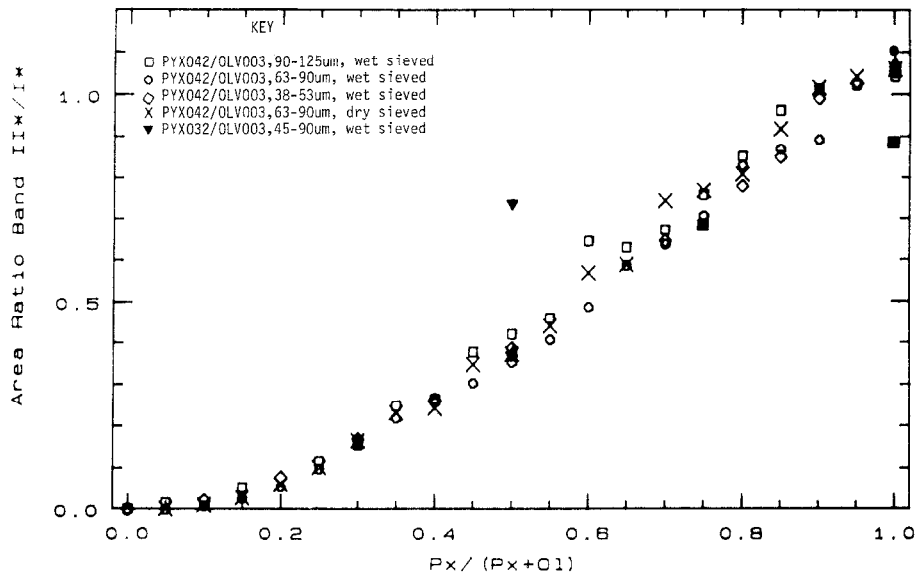


Fig. 10. Plot of the area ratio (band II*/band I*) for olivine-orthopyroxene mixtures as a function of orthopyroxene abundance. There are no apparent variations due to changes in grain size. Points which deviate substantially from the trend are for non-equilibrium mixtures.

in Gaffey (1976) and Feierberg *et al.* (1982). A number of spectral-compositional relationships have been found. The most effective spectral deconvolution technique involves determining the relative end member abundances from the ratio of the area of band II* to band I* (Figure 1). The usefulness of this band area ratio arises from the fact that only pyroxene has an absorption band near 2 $\mu$m. As OPX content increases, the band II* area increases and a roughly linear relationship exists with OPX abundance (Figure 10). The ferrous iron contents of the two phases can be determined from the wavelength position of the band I minimum after end member abundances have been obtained. This arises from the fact that the band I minimum wavelength position is a function of both end member abundances and ferrous iron contents. The band moves to longer wavelengths with increasing olivine abundance as well as increasing ferrous iron content (Gaffey, 1976; Singer, 1981; Cloutis *et al.*, 1986). The wavelength position of band I has been measured as a function of end member abundances for a range of mafic silicate compositions. The data, irrespective of grain size, show a tightly constrained trend for equilibrium OPX-OLV assemblages (Figure 11). Once end member abundances have been determined from the band area ratio (Figure 10), the band minimum wavelength position can be plotted in the field of Figure 11 at the predetermined end member abundance ratio. Then, the curve fitting the data of Figure 11 (not shown) can be shifted up or down until it overlies the point for the mixture. The $Fe^{2+}$ content of the end members can then be read off the left and right vertical scales where the curve intersects the heavy black vertical lines indicating ferrous iron content. Such complex deconvolution procedures are re-

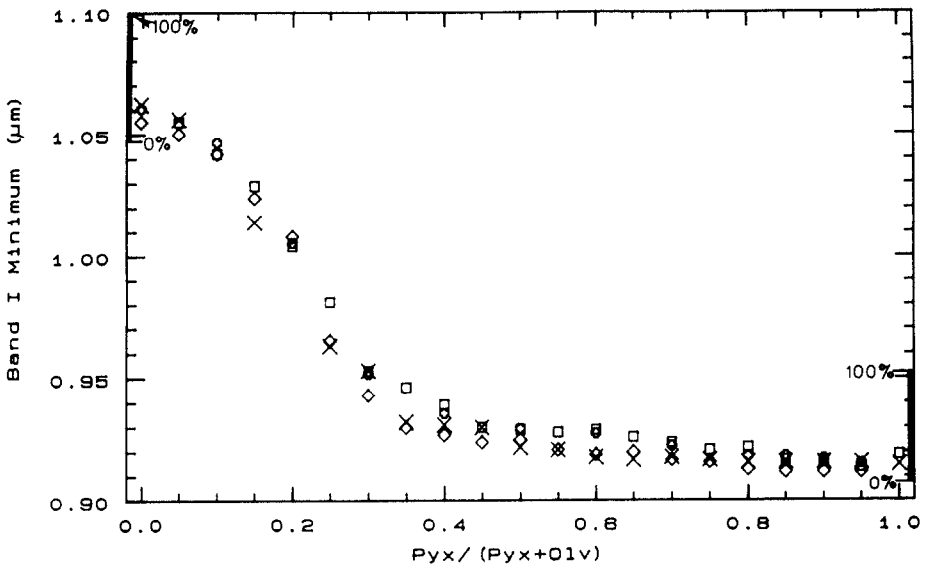


Fig. 11. The variation of the wavelength position of the band I minima as a function of orthopyroxene abundance. The heavy vertical lines on either side of the scale indicate the range of possible band positions for the end members as a function of ferrous iron content (from Cloutis *et al.*, 1986).

quired because intimate mineral mixtures are not simple linear combinations of the end member spectra (Figure 12).

The addition of olivine to orthopyroxene causes a number of other spectral effects which have not been rigorously quantified. A number of these effects are given in Cloutis *et al.* (1986). The most apparent of these is the shift of the interband peak (Figure 1) to longer wavelengths with increasing olivine content (Feierberg *et al.*, 1982).

### 4.2. Orthopyroxene + clinopyroxene spectra

Orthopyroxene + clinopyroxene mixture spectra have not been as intensively studied as those of OPX + OLV (Adams, 1974; Singer, 1981; Johnson *et al.*, 1983; Cloutis, 1985; Sunshine *et al.*, 1990). The ensuing discussion is restricted to those mixtures containing spectral type B clinopyroxenes because this spectral type encompasses the Ca-deficient samples which are more common than type A in mafic assemblages (Papike, 1980). OPX-CPX spectra are more difficult to analyze than OPX-OLV spectra because both OPX and CPX exhibit absorption bands near 1 $\mu$m (band I) and 2 $\mu$m (band II; Figure 13). A number of techniques can be applied to deconvolution of their spectra. The absorption feature near 1 $\mu$m contains contributions by both the OPX and CPX. Analysis of this feature indicates that OPX tends to dominate the spectrum in this wavelength region; i.e. the wavelength position of this band in a 50 : 50 OPX : CPX mixture is skewed towards OPX (Figure 14). In general, a greater separation exists between the OPX and CPX band II. Consequently, mixture spectra will frequently display two partially

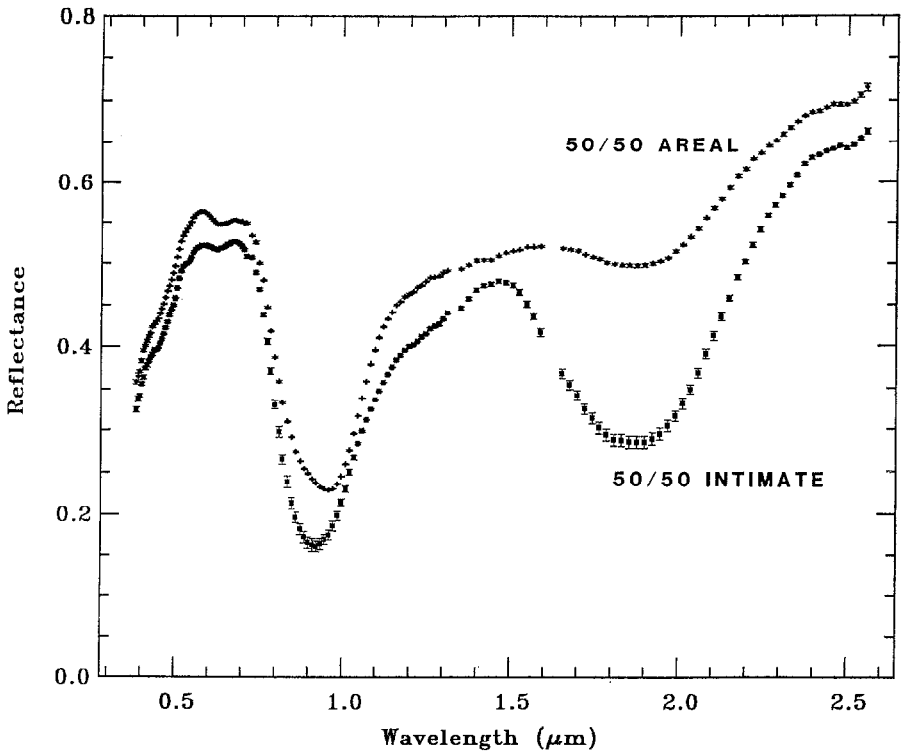


Fig. 12. Reflectance spectra of an intimate and areal (mathematical average) of 50% olivine (OLV003) and 50% orthopyroxene (PYX042).

resolvable absorption bands in the 2 $\mu$m region (Figure 13). This wavelength region is also useful because it is not overlapped by absorption bands due to common accessory phases such as plagioclase, olivine, or opaques. It is usually possible to identify the presence of two pyroxenes by the appearance of two absorption bands in this wavelength region, particularly for mixtures containing ~50–90% CPX (Figure 13). The partial overlap of these bands results in both band II minima being shifted to values intermediate between those of the pure end members; clinopyroxene bands being shifted to shorter wavelengths and the orthopyroxene band being shifted to longer wavelengths (Figure 14). Even in the absence of more sophisticated curve resolving techniques, band II positions can be used to at least constrain pyroxene compositions using the data in Figure 4. For OPX/CPX abundances in the 40 : 60 to 15 : 85 range, band II is of approximately equal strength for both phases, allowing the OPX : CPX ratio of an assemblage to be rapidly constrained.

OPX and type B CPX spectra are superficially similar but there are a number of differences which are potentially useful for spectral deconvolution but which have not been rigorously quantified. The wavelength positions of the OPX band I (~0.9–0.94 $\mu$m), band II (~1.8–2.1 $\mu$m) and the interband peak (1.23–1.40 $\mu$m)

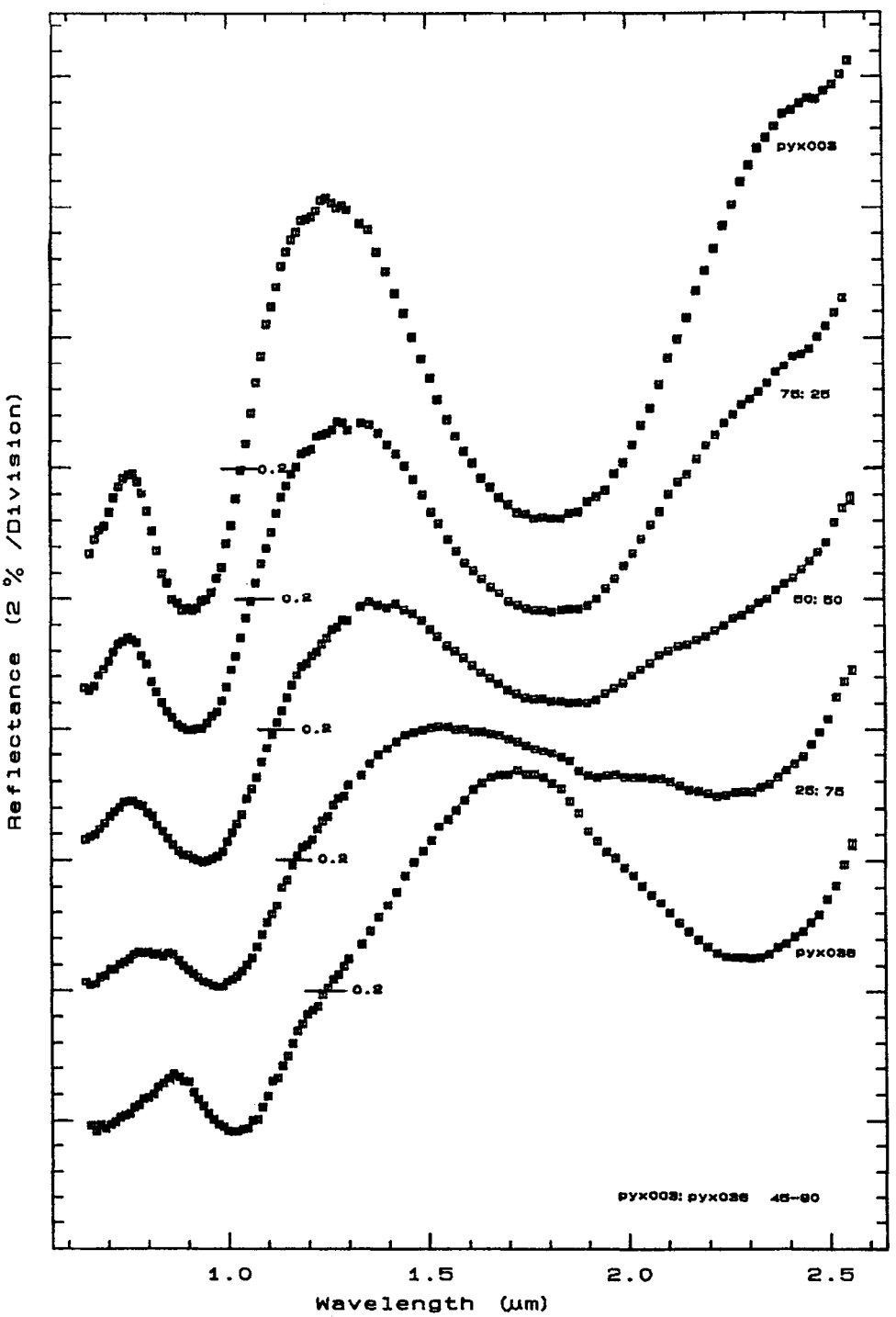


Fig. 13. Reflectance spectra of an orthopyroxene-clinopyroxene mixtures series involving PYX003 and PYX036 (measured at UH).

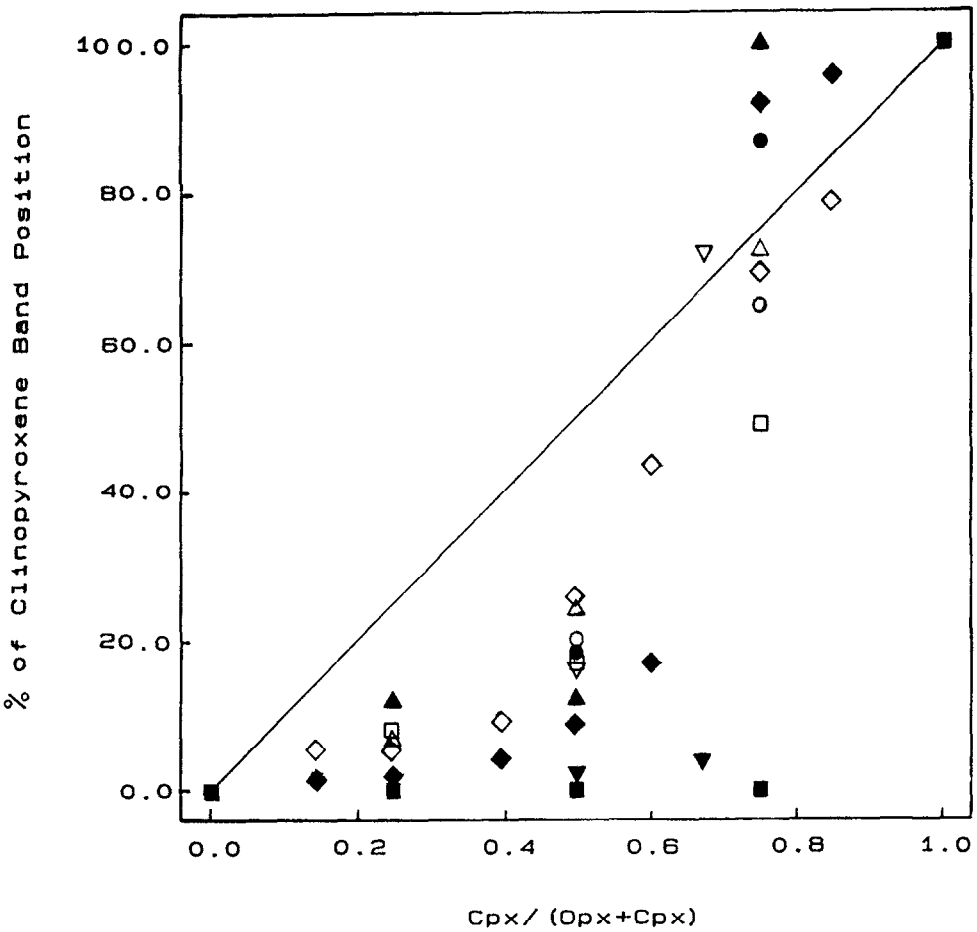


Fig. 14. Plot of the percent change in orthopyroxene band I and band II minima wavelength positions as a funcion of clinopyroxene content for various OPX-CPX mixtures. Open symbols = band I minima, filled symbols = band II minima. Squares = PYX032 + PYX040; circles = PYX003 + PYX036; upright triangles = Singer (1981); inverted triangles = Adams (1974); diamonds = Sunshine *et al.* (1990). In each case the wavelength position of the orthopyroxene is set to zero and the clinopyroxene to 100% for each series in order to remove the effects of different band positions of the end members for each series.

differ from those for CPX (~0.96–1.05 $\mu$m; ~2.1–2.4 $\mu$m, ~1.5–2.0 $\mu$m, respectively). Other differences are found in terms of the reflectance ratio of the 0.7 $\mu$m peak to band II (1.0–3.0 – OPX, 0.4–1.2 – CPX), and the wavelength position of the tangent intercept (Figure 1; 1.0–1.1 $\mu$m – OPX, 1.09–1.43 $\mu$m – CPX).

The most promising techniques for deconvolving OPX + CPX spectra are based on curve fitting/resolving methods (Sunshine *et al.*, 1990) and semi-empirical approaches (Johnson *et al.*, 1983). Recent work in this area shows that a modified Gaussian fit to the absorption features allows the component absorption bands to be identified and their wavelength positions to be determined (Sunshine *et al.*,

1990). As mentioned, band wavelength positions are very diagnostic indicators of major cation abundances.

### 4.3. Clinopyroxene + olivine spectra

Clinopyroxene + olivine spectra are the least studied of the two-component mafic silicate mixtures (Singer, 1981; Johnson *et al.*, 1983; Miyamoto *et al.*, 1983; Cloutis, 1985). Effective spectral deconvolution procedures are hampered by the lack of laboratory data for these mixtures and by the natural spectral diversity of clinopyroxenes. Procedures based on band area ratios and band wavelength positions are somewhat imprecise because of these factors. Even the most effective semi-empirical spectral analysis techniques (Johnson *et al.*, 1983) require a knowledge of the spectral properties of the end members, which, for clinopyroxenes, are often difficult to predict from compositional information alone.

Clinopyroxenes do differ from olivines in a number of important respects, such as band I minimum wavelength position (0.96–1.06 $\mu$m: CPX, ~1.05–1.09 $\mu$m: OLV), wavelength position of the tangent intercept (~1.09–1.2 $\mu$m: CPX, 1.45–1.6 $\mu$m: OLV), and wavelength position of the 0.7 $\mu$m peak (~0.8 $\mu$m: CPX, ~0.5–0.7 $\mu$m: OLV). In addition, band II is absent in olivine. This is significant because the presence of even small amounts of clinopyroxene mixed with olivine will be readily apparent (e.g. Cloutis *et al.*, 1990b). Band II*/I* area ratios less than 0.1 generally indicate clinopyroxene abundances of <40%. The most useful spectral parameter seems to be the use of the tangent intercept. Values for this intercept for all available mixtures have been assembled and used to construct the trend shown in Figure 15. The area between the two curves defines the region occupied by CPX-OLV mixtures. End member abundance determinations can also be checked by examining the wavelength position of the local reflectance maximum in the 0.5–0.8 $\mu$m region. When olivine and clinopyroxene are present in subequal amounts, this wavelength region generally exhibits a flat broad peak across this wavelength range because the spectral contributions by both phases are approximately equal for equal abundances.

### 4.4. Mafic silicate + plagioclase feldspar spectra

Two-component mixtures of mafic silicates and plagioclase feldspar have been spectrally characterized by Adams (1974), Nash and Conel (1974), McFadden and Gaffey (1978), and Crown and Pieters (1987). The reflectance spectrum of a 71.4/28.6 OPX/PLG mixture (sample (L25 – Table III) and the end member spectra are shown in Figure 16. Comparison of the curves indicates that the addition of an appreciable amount of plagioclase has little effect on the shape of the pyroxene spectrum. This is because the plagioclase absorption band is much weaker than that of the pyroxene (McFadden and Gaffey, 1978). The most noticeable effects are an increase in overall reflectance and a more pronounced asymmetry on the short wavelength side of the interband peak. The former effect can be attributed to the increase in scatter caused by the inclusion of the relatively

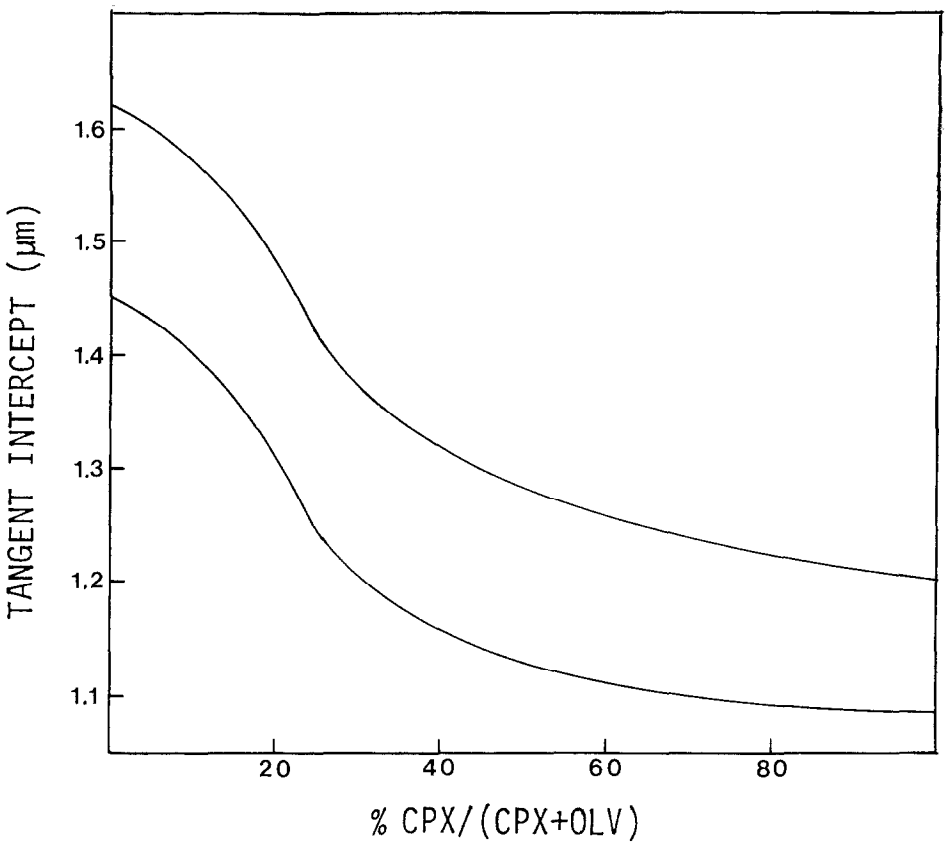


Fig. 15. Wavelength position of the intercept of a horizontal line tangent to the reflectance spectra at the local reflectance maximum near 0.7 $\mu$m with the long wavelength wing of band I (tangent intercept in Figure 1), for various clinopyroxene-olivine mixtures. All data points lie between the two curves.

transparent plagioclase (Morris, 1985). Even though the main plagioclase absorption band occurs in the same wavelength region as the interband peak, plagioclase abundance is not sufficient to cause a noticeable shift in position (Table II). However, the band area ratio is somewhat higher for L25 presumably because the overall reflectance increase, caused by the presence of plagioclase, results in a lower 0.7 $\mu$m peak: interband peak reflectance ratio. When this decreased ratio is divided into the band II*/band I area ratio, a higher value results (Figure 18). At high plagioclase abundances ($\geq$60%) the initial increase in II*/I* area ratio turns into a decrease as the plagioclase becomes more spectrally dominant (Figure 18). Band minima wavelength positions are relatively unchanged between the pure orthopyroxene and L25. Plagioclase has almost no effect on the pyroxene absorption band wavelength positions at abundances of <75% (Figure 17; Table II). The detectability of plagioclase in a mixture is also dependent on grain size (Adams and Charette, 1975; Crown and Pieters, 1987). In general the presence of plagioclase can first be inferred by the flattening or shift of the interband peak.

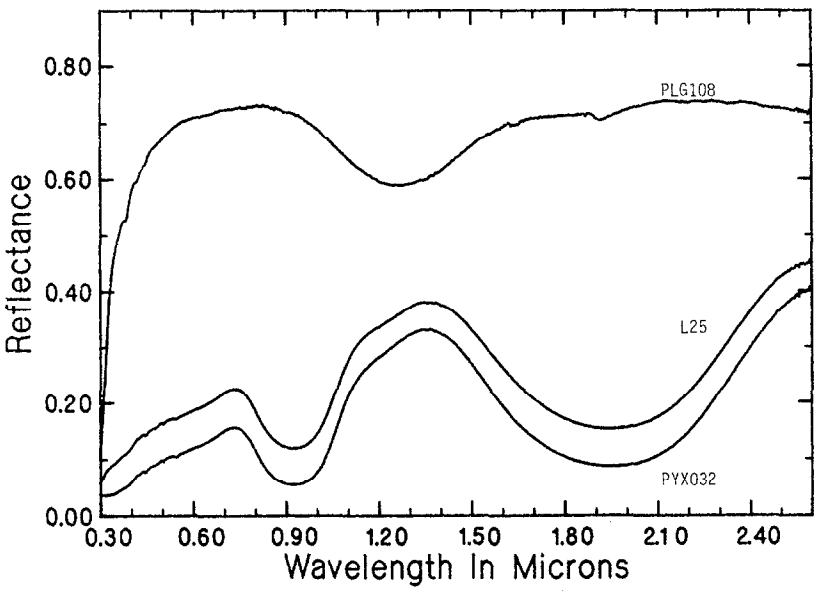


Fig. 16. Reflectance spectra (0.3–2.6 $\mu$m) of sample L25, a 71.4/28.6 PYX/PLG mixture (45–90 $\mu$m grain size), and the pure end members (PYX032, PLG108). Spectra measured at RELAB ($i = 30°$, $e = 0°$).

Only when plagioclase abundance reaches ~75% is its absorption band clearly resolvable.

Neither the increase in overall reflectance nor the shift of the pyroxene interband peak can be rigorously quantified to yield pyroxene : plagioclase ratios. The former effect can be simulated by decreasing the grain size of either phase or by decreasing the amount of opaques which may be present (Crown and Pieters, 1987). The wavelength position of the interband peak varies in pyroxenes without the presence of plagioclase being required and the slightly asymmetric appearance of it can be reproduced by the addition of small amounts of olivine (Cloutis, 1985). Thus, quantitative determinations of plagioclase abundance in mafic silicate-bearing mixtures is very imprecise using the 0.3–2.6 $\mu$m region. Further uncertainties are inherent in the analysis of the reflectance spectra of planetary surfaces such as the moon because the plagioclase absorption band becomes weaker if the mineral is subjected to shock (Adams *et al.*, 1979; Bruckenthal and Pieters, 1985).

### 4.5. Silicate + opaque mineral mixtures

While the overall reflectance of mafic silicates increases with decreasing particle size, the opposite trend is observed for opaque minerals such as magnetite and ilmenite (Hunt *et al.*, 1971). Spectral reflectance studies of mafic silicate + opaque mixtures indicate that even a few percent of a fine-grained dispersed opaque is very effective at reducing overall reflectance (Nash and Conel, 1974; Pieters, 1983; Cloutis *et al.*, 1990a,c).

TABLE II

Various spectral parameters of some of the mineral mixtures used in this study

| Sample | Band minima | | Band centers | | Interband | Area | Band depths | |
|---|---|---|---|---|---|---|---|---|
| | I | II | I | II | peak | ratio | I | II |
| | | | | Olivine/magnetite | | | | |
| 100/0 | 1.056 | – | 1.060 | – | – | 0 | 70 | – |
| 90/10 | 1.057 | – | 1.058 | – | – | 0 | 50 | – |
| 90/10[1] | 1.056 | – | 1.059 | – | – | 0 | 38 | – |
| 50/50 | 1.056 | – | 1.061 | – | – | 0 | 32 | – |
| 0/100 | 1.025 | – | 1.101 | – | – | 0 | 26 | – |
| | | | | Pyroxenes | | | | |
| PYX032 | 0.921 | 1.949 | 0.934 | 1.981 | 1.36 | 0.96 | 6.10 | 4.00 |
| PYX036 | 1.020 | 2.299 | 1.031 | 2.339 | 1.73 | 0.43 | 5.27 | 1.76 |
| | | | | Mineral mixtures | | | | |
| L3 | 0.925 | 1.946 | 0.935 | 1.989 | 1.35 | 1.14 | 2.93 | 2.29 |
| L9 | 0.926 | 1.963 | 0.938 | 2.009 | 1.36 | 1.42 | 1.96 | 1.81 |
| L12 | 0.922 | 1.950 | 0.932 | 1.988 | 1.35 | 1.23 | 2.19 | 1.86 |
| L15 | 0.977 | 1.947 | 0.983 | 1.980 | 1.49 | 0.36 | 2.13 | 1.39 |
| L18 | 0.922 | 1.950 | 0.935 | 1.987 | 1.37 | 1.07 | 4.17 | 2.98 |
| L21 | 0.925 | 1.947 | 0.936 | 1.987 | 1.38 | 1.19 | 2.00 | 1.72 |
| L24 | 1.020 | 2.298 | 1.039 | 2.359 | 1.73 | 0.54 | 2.90 | 1.45 |
| L25 | 0.923 | 1.946 | 0.937 | 1.991 | 1.36 | 1.16 | 3.20 | 2.51 |

Band minima, centers, and interband peak positions are given in microns.
Area ratio (Column 7) is band II*/band I*.
Band depths (columns 8 and 9) are in percent.
Band depths for olivine/magnetite series are the ratio of the reflectance at 1.8 $\mu$m to the reflectance of the band I minimum. Band I and band II depths for pyroxenes and mineral mixtures are the ratio of the reflectance of the interband peak to the band I minimum and ratio of the interband peak to the band II minimum, respectively.

TABLE III

Proportions of the various end members used in the mineral mixtures

| Mixture | PYX032 | PYX036 | PLG108 | OLV003 | ILM101 |
|---|---|---|---|---|---|
| L3 | 66.6 | 0.0 | 26.7 | 0.0 | 6.7 |
| L9 | 66.6 | 0.0 | 26.7 | 0.0 | 6.7 |
| L12 | 53.4 | 0.0 | 21.3 | 0.0 | 25.3 |
| L15 | 28.6 | 0.0 | 11.4 | 57.1 | 2.9 |
| L18 | 85.7 | 0.0 | 11.4 | 0.0 | 2.9 |
| L21 | 37.0 | 0.0 | 59.3 | 0.0 | 3.7 |
| L24 | 0.0 | 66.6 | 26.7 | 0.0 | 6.7 |
| L25 | 71.4 | 0.0 | 28.6 | 0.0 | 0.0 |

All mixtures contain 45–90 $\mu$m grain size minerals except sample L9 which contains <45 $\mu$m sized plagioclase (PLG108).
All abundances are in weight percent.

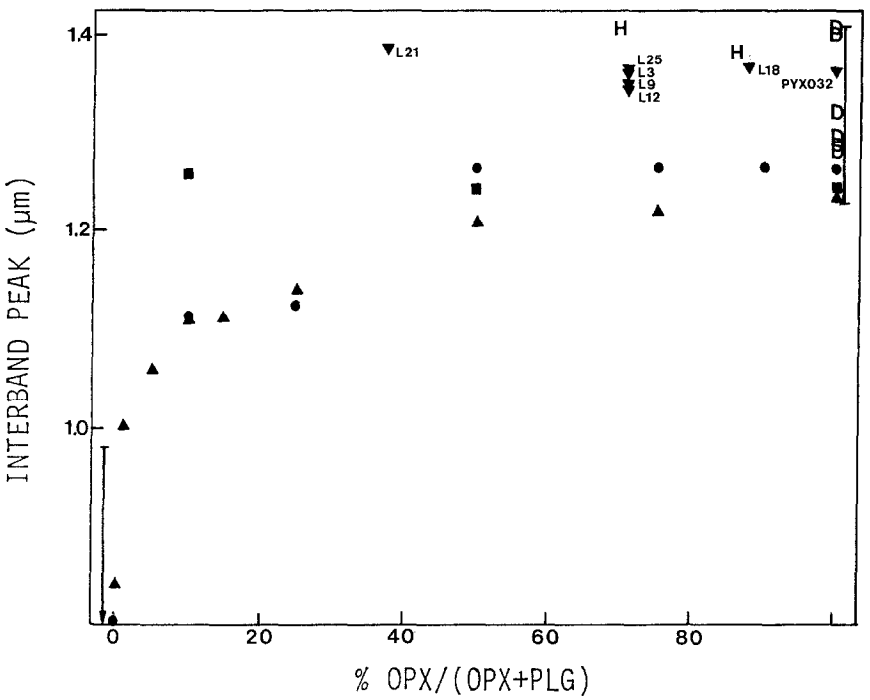


Fig. 17. Wavelength positions of the reflectance maximum between band I and band II (interband peak – Figure 1) for various orthopyroxene-plagioclase assemblages as a function of plagioclase content. Squares = Adams (1974); upright triangles = Nash and Conel (1974); circles = Mustard *et al.* (1986); D = diogenites (McFadden *et al.*, 1982; Gaffey, unpublished); H = howardites (Gaffey, unpublished); inverted triangles = this study. Vertical lines at 0 and 100% indicate interband peak wavelength position range for pure plagioclase and pure orthopyroxene, respectively.

The band depth criterion, $D_b$ (Clark and Roush, 1984), is useful for assessing the darkening effect of magnetite. Olivine band depths are influenced by both the abundance and grain size of the magnetite (Figure 19). The 90/10 OLV/MAG spectrum (45–90 $\mu$m grain size) has a band depth of 50% (Table II). A simple average of the pure end member band depths is 66%. The lower than expected value for the mixture indicates that magnetite suppresses band depths beyond what one would expect from its abundance. The band depth value for a similar 90/10 OLV/MAG mixture, containing <45 $\mu$m grain size magnetite is even lower (Table II). Thus, reducing opaque grain size is even more effective at suppressing mafic silicate absorption bands.

Overall reflectance values also indicate the larger than expected influence of magnetite. Such values are most useful for estimating mafic silicate grain sizes in opaque-free assemblages (Cloutis *et al.*, 1986, 1990b) but the presence of opaques lowers overall reflectance, simulating an increase in mafic silicate grain size. Taking the absolute reflectance at 0.56 $\mu$m as an example, the average for 90% OLV and 10% MAG is 0.665. The value for the mixture is 0.362. Consequently, overall reflectance will provide only a lower limit on the mean grain size of mafic silicates

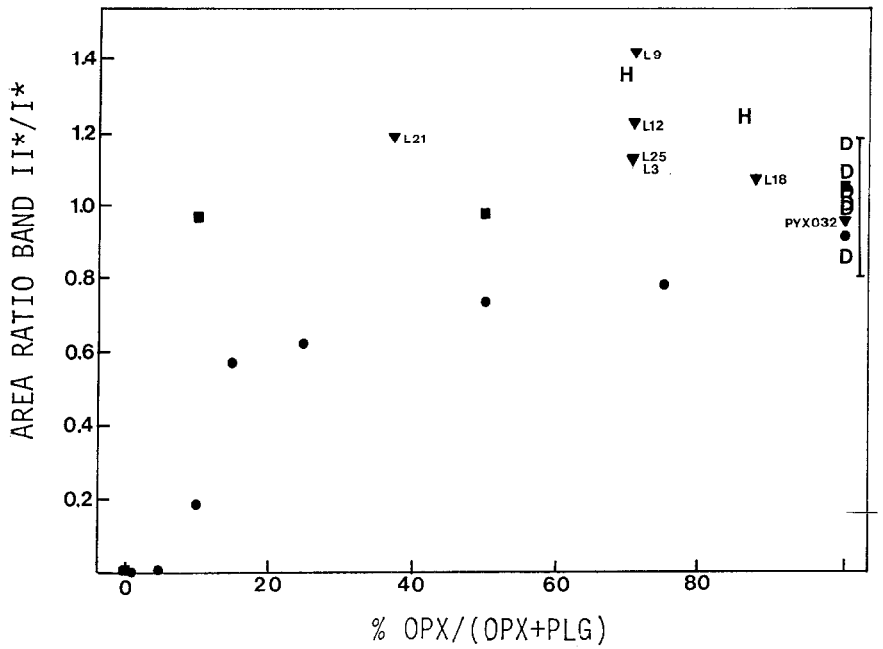


Fig. 18. Band II*/band I* area ratio (see text for details) for various orthopyroxene-plagioclase assemblages. Symbols and data sources are the same as for Figure 17.

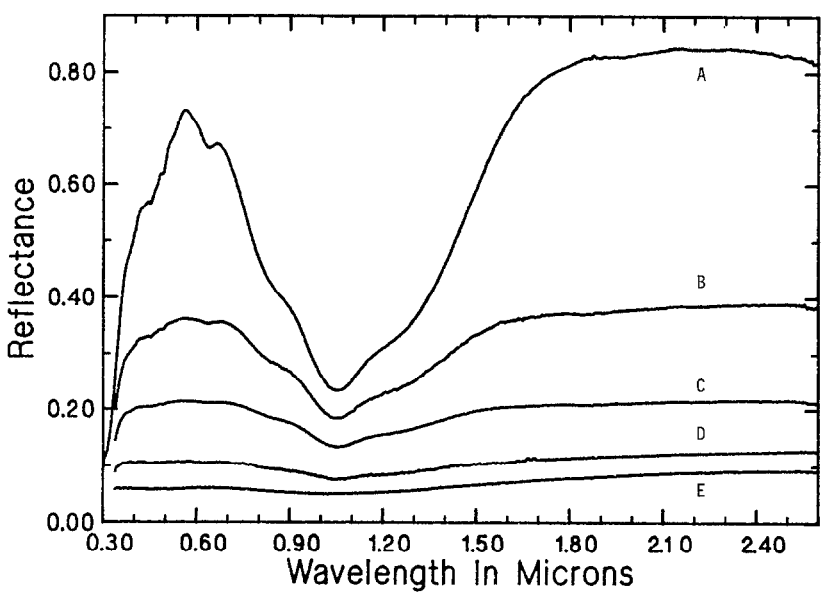


Fig. 19. Reflectance spectra of some olivine + magnetite mixtures. Respective olivine and magnetite abundances are 100/0 (A), 90/10 (B), 90/10 (C), 50/50 (D), and 0/100 (E). All mixtures contain 45–90 $\mu$m sized minerals except (C) which contains $<45$ $\mu$m size magnetite. Spectra measured at RELAB ($i = 0°$, $e = 15°$).

if opaques are present. Significantly, both the olivine band I center wavelength position, after removal of a straight line continuum, and the band I minimum, are relatively unaffected by the presence of magnetite (Table II).

The spectral data for pyroxene + magnetite mixtures are scanty but suggest that band area ratios are largely unaffected by the presence of $\leqslant$10% magnetite, even though band depths are reduced (Pieters, 1983). Band minima wavelength positions are also minimally affected by the presence of neutral opaques at the few tens of percent level. Substantial amounts of magnetite or ilmenite are required ($\geqslant$50%) to significantly affect band positions (Nash and Conel, 1974; Pieters, 1983; Cloutis *et al.*, 1990b). Since band area ratios and band positions are among the most diagnostic mafic silicate spectral parameters, little compositional information is lost due to the presence of opaques. The major effect of opaques is to introduce uncertainties into grain size determinations.

## 5. Three Component Mixtures

Systematic spectral reflectance data for ternary mixtures involving mafic silicates are scarce (Nash and Conel, 1974; Mustard and Pieters, 1989). The spectral reflectance systematics of such assemblages can be inferred from these studies and the data for two-component mixtures. Ternary mixtures basically involve mafic silicates with plagioclase and/or opaques, or three mafic silicate mixtures (OLV + OPX + CPX). As mentioned, plagioclase abundances below ~75% are difficult to unambiguously identify, although the presence of lesser amounts of plagioclase can best be inferred from its effect on the interband peak and band area ratio of pyroxene.

### 5.1. Plagioclase-bearing, opaque-free mixture spectra

These mixtures include OPX + CPX + PLG, OPX + OLV + PLG, and CPX + OLV + PLG. The spectral systematics of such mixtures are basically the same as those for two mafic silicate assemblages with the addition of a relatively transparent phase (plagioclase), whose most noticeable effect is on the interband peak of pyroxene. Application of a simplified bidirectional reflectance model (Hapke, 1981) indicate that OPX + OLV + PLG mixtures can be deconvolved into their component phases with an accuracy of a few percent (Mustard and Pieters, 1989), provided the spectral properties of the end members are known. Empirically, such assemblages can best be interpreted on the basis of binary mafic silicate mixtures with allowances made for the presence of plagioclase.

### 5.2. Plagioclase- and opaque-bearing mixture spectra

These mixtures involve any one of the three mafic silicates (OLV, OPX, CPX) mixed with plagioclase and an opaque phase. Once again, these mixtures can largely be modelled on the basis of binary mixtures (mafic silicates + opaques) because of the relative transparency of plagioclase. The reflectance spectrum of a

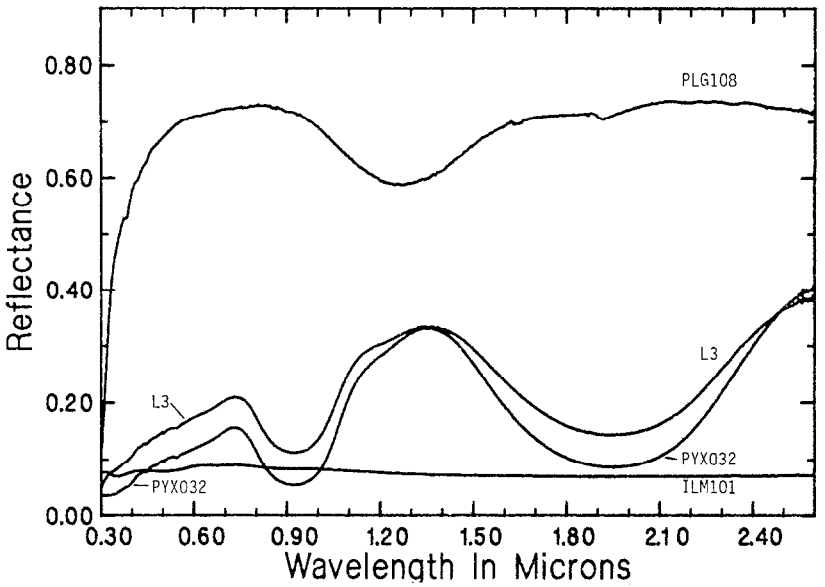


Fig. 20. Reflectance spectra of sample L3 and the various end members. See Table III for mineral proportions in L3 and Table I for compositions of the end members. Spectra measured at RELAB ($i = 30°$, $e = 0°$).

66.7/26.7/6.7 OPX/PLG/ILM (45–90 $\mu$m grain size) is shown in Figure 20 (sample L3). Comparison of the mixture to the various components can be used to illustrate the relative spectral importance of each phase. The overall reflectance of the mixture is higher than the pure orthopyroxene and band depth is reduced (Table II) because of the presence of the plagioclase but is partially offset by the presence of ilmenite. This effect can also be seen by comparing spectra L3 and L25 (Figure 16). The presence of plagioclase is best inferred by how it imparts an asymmetric appearance to the pyroxene interband peak. Neither the ilmenite nor the plagioclase have any noticeable effect on the wavelength position of the pyroxene absorption bands. Thus, pyroxene composition can still be determined using band position criteria.

The effect of varying plagioclase grain size is illustrated in Figure 21. Both L3 and L9 contain the same end member abundances (Table III). Mixture L9 contains $<45$ $\mu$m sized plagioclase while mixture L3 contains 45–90 $\mu$m sized plagioclase. The presence of fine-grained plagioclase leads to an increase in the ratio of scattered to absorbed light, resulting in reduced band depths and increased overall reflectance (Table II). Band positions are at slightly higher wavelengths but this difference is considered to be insignificant. Band area ratio (II*/I*) is significantly higher (Table II). Again, this can best be explained by an increase in overall reflectance due to the addition of plagioclase which effectively decreases the

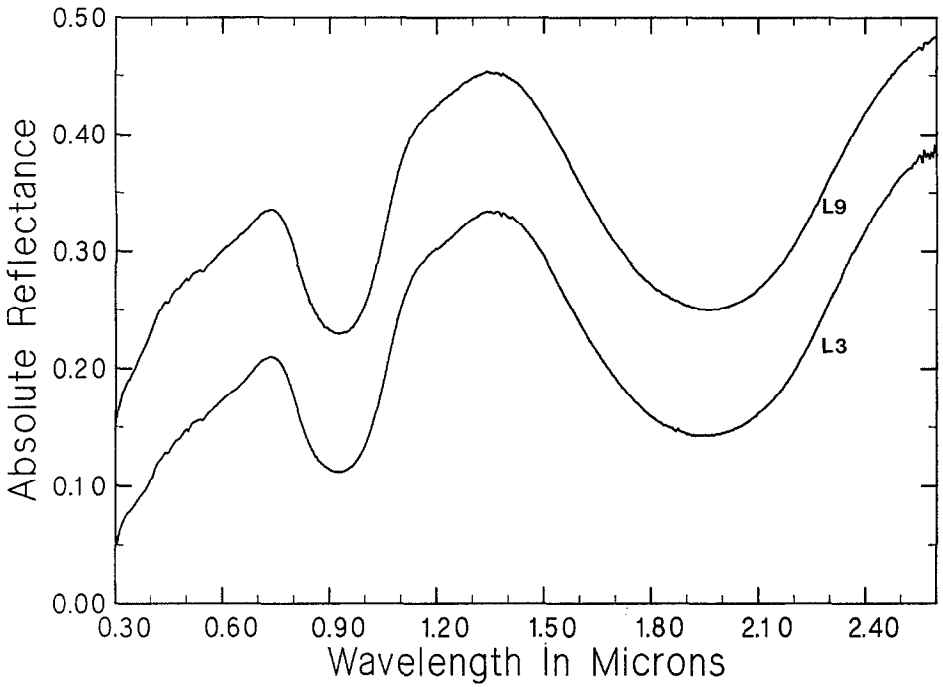


Fig. 21. Reflectance spectra of sample L3 which contains 45–90 $\mu$m sized grains, and sample L9 which contains <45 $\mu$m sized plagioclase. Mineral abundances are the same in both (Table III). Spectra measured at RELAB ($i = 30°$, $e = 0°$).

0.7 $\mu$m peak: interband peak ratio and consequently increases the II*/I* area ratio.

The asymmetric appearance of the interband peak is more apparent in the coarser-grained plagioclase sample (L3). While higher overall reflectance of spectrum L9 may suggest the presence of fine-grained plagioclase, its identification is hampered because it imparts less of an asymmetry to the interband peak. There is no difference in wavelength position of the interband peak (Table II).

Varying the relative abundances of one of the end members also affects reflectance spectra. The reflectance spectra of four OPX + PLG + ILM spectra (L3, L12, L18, L21) and a CPX + PLG + ILM spectrum (L24) are shown in Figure 22. All mixtures contain 45–90m sized grains and the proportions are given in Table III. The spectral effects of increasing opaque abundance is illustrated by comparing curves L3 and L12. These mixtures have been prepared such that the OPX/PLG ratio is unchanged. The effect of increasing opaque abundance is to lower both overall reflectance and band depths while the band area ratio increases slightly (Table II).

Varying the silicate ratio is illustrated using spectra L3, L18 and L21 (Figure 22). L3 and L18 have the same PLG/ILM ratio and L3 and L21 have the same OPX/ILM ratio. L18 relative to L3 shows the expected effects of increasing pyroxene abundance- band positions and band areas are relatively unchanged

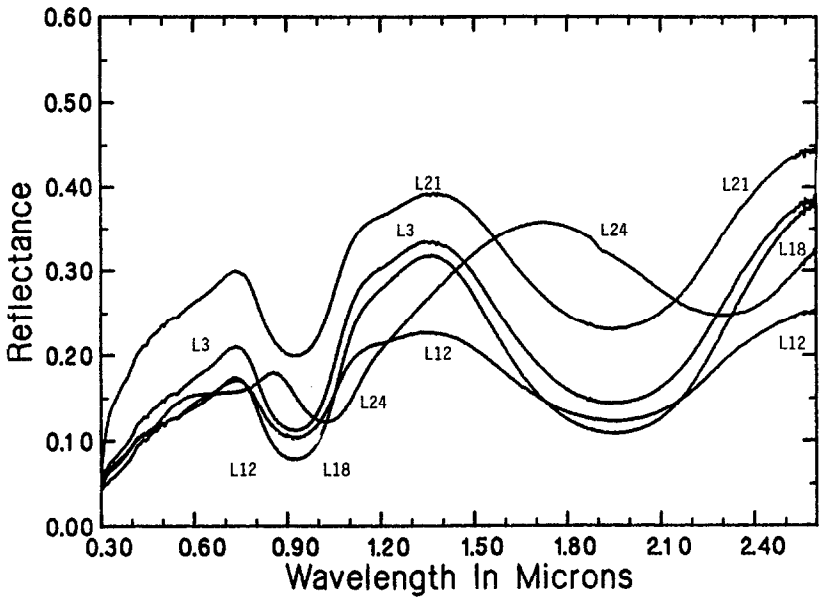


Fig. 22. Reflectance spectra of samples L3, L12, L18, L21, and L24 (measured at RELAB; $i = 30°$, $e = 0°$).

while band depths are reduced and overall reflectance is higher in the latter. Increasing pyroxene abundance simulates some, but not all, of the effects of decreasing opaque abundance – greater band depths, unchanged band positions and band areas (Table II).

Sample L21 differs from L3 by its greater plagioclase abundance. As previously discussed, increasing plagioclase abundance leads to greater overall reflectance, decreased band depths, and almost no change in band positions (Table II). The increase in band area ratio is not great because the plagioclase abundance (59%) is in the region of Figure 18 where area ratios begin to decline after the initial increase with increasing plagioclase content.

The spectral changes inherent in varying pyroxene composition are also illustrated in Figure 22. Sample spectra L3 and L24 have identical phase abundances but L3 contains PYX032, an orthopyroxene, while L24 contains PYX036, a clinopyroxene (Table I). The differences are readily apparent in terms of changes in all important spectral parameters such as overall reflectance, band positions and depths and band area ratios. Such widespread changes serve to emphasize the point that mafic silicates are frequently the most conspicuous spectral phase and that varying the composition of this one component results in changes in most key spectral parameters.

### 5.3. Opaque-bearing, plagioclase-free mixture spectra

These mixtures encompass any two of the three mafic silicates (OPX, CPX, OLV) mixed with an opaque phase. They can best be interpreted as two-component mafic silicate mixtures modified by the presence of opaques. The binary mafic

silicate mixtures have already been dealt with, as have mafic silicate + opaque mixtures. The most fruitful avenue of spectral analysis thus involves using the spectral interpretation techniques for binary mafic silicate mixtures because opaques do not significantly affect the key spectral parameters outlined above. Grain size determinations will be hampered by the presence of opaques and consequently only lower limits on grain size may be obtained.

### 5.4. Plagioclase- and opaque-free mixture spectra

The only ternary group in this category is OPX + CPX + OLV. Unfortunately, systematic studies of such assemblages have not yet been undertaken. Ternary assemblages depleted in one of the three components (e.g. $\leq$15%) can effectively be analyzed as two-component mixtures bearing in mind the presence of the third phase and its possible effects on spectral parameters. Certain spectral features can be used to at least constrain end member properties even in the absence of systematic deconvolution procedures. The presence of orthopyroxene can best be inferred on the basis of an absorption feature in the ~1.8–2.1 $\mu$m region, clinopyroxene by the presence of an absorption band in the ~2.1–2.4 $\mu$m region and a reflectance peak near 0.8 $\mu$m, and olivine by the presence of two absorption features near 0.9 and 1.2 $\mu$m and a broadening of the main absorption band near 1 $\mu$m. OPX/CPX ratios can best be determined by analysis of their absorption bands in the 2 $\mu$m region (band II) as outlined for binary OPX + CPX mixtures because olivine is spectrally neutral in this wavelength region. The relative strengths of each of the diagnostic features outlined above can be used to place severe constraints on phase abundances even in the absence of quantitative calibrations. Further work is required to establish such quantitative guidelines.

## 6. Four Component Mixture Spectra

M-UM assemblages are considered here as mixtures of up to five possible components (OPX, CPX, OLV, PLG, MAG or ILM), so that five possible four-component assemblages are conceivable. Opaque-free assemblages are similar to the previously discussed ternary mixtures of OPX + CPX + OLV, with allowances made for plagioclase which is spectrally difficult to detect and which has only a minor effect on mafic silicate absorption features at low to moderate abundances. Plagioclase-free mixtures can similarly be analyzed using the appropriate ternary systems with allowances made for the opaques, which as mentioned, do not appreciably affect most key spectral parameters. Orthopyroxene-free mixture spectra will be dominated by the clinopyroxene and olivine with opaques lowering overall reflectance and plagioclase increasing it and perhaps imparting an asymmetry to the interband peak. Again, the mafic silicate spectral parameters such as band area ratios and band positions should be relatively unaffected. Olivine-free mixture spectra will be dominated by the pyroxenes and are effectively analyzed

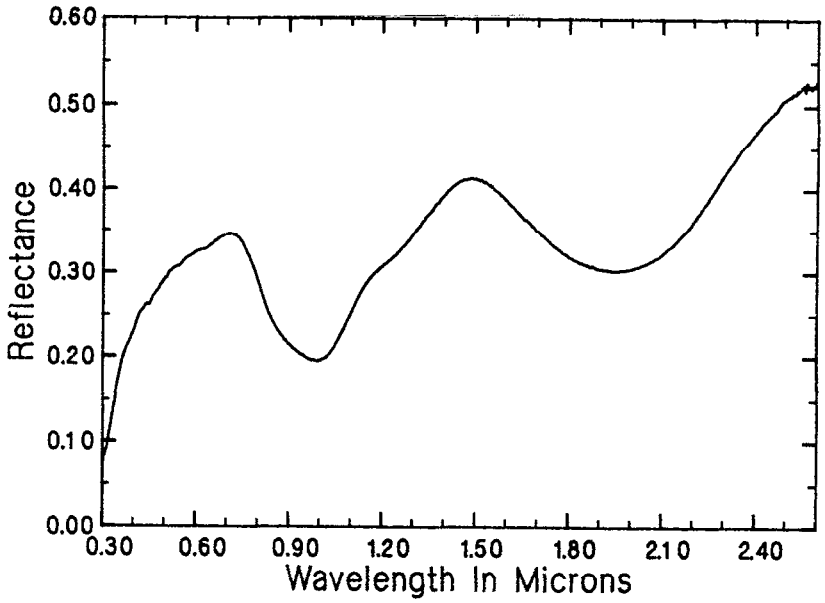


Fig. 23. Reflectance spectrum of sample L15. See Table III for mineral abundances. Spectrum measured at RELAB ($i = 30°$, $e = 0°$).

using two-pyroxene criteria with the above mentioned allowances made for plagioclase and opaques.

The same rationale can be applied to clinopyroxene-free mixture spectra. Such a spectrum is shown in Figure 23. The sample, L15, contains 28.6/57.1/11.4/2.9 OPX/OLV/PLG/ILM. The OPX/OLV ratio is such that both phases are of approximately equal intensity in the 1 $\mu$m region (Cloutis *et al.*, 1986). In spite of the high olivine abundance, the orthopyroxene band II is readily apparent. The broadness of band I and the presence of inflections near 0.9 and 1.2 $\mu$m are characteristic of the olivine. The presence of plagioclase is not obvious given its low abundance (11.4%) and the presence of olivine, but the high overall reflectance is suggestive of plagioclase. The ilmenite is also not apparent because of its low abundance, the offsetting effects of the plagioclase, and its lack of well-defined absorption bands. Thus, such a four-component mixture could be spectrally analyzed using calibrations for OPX + OLV assemblages with almost no loss of compositional information.

## 7. Five Component Mixture Spectra

This assemblage contains all five components, OPX + CPX + OLV + PLG + ILM/MAG and, following previous arguments, will be dominated by the mafic silicate absorption bands with plagioclase and opaques raising and lowering overall reflectance, respectively. A five-component assemblage has not been spectrally characterized, but should be similar in appearance to that shown in Figure 23,

exhibiting readily apparent mafic silicate absorption bands. The degree of spectral modification by plagioclase and opaques will depend on their abundances, grain sizes, and degree of dispersion.

## 8. Discussion

Analysis of extant and newly generated spectral data indicates that as more components are added to a mixture, the quality and quantity of compositional information which can be derived from spectral analysis diminishes. The reflectance spectra of increasingly complex mixtures remain dominated by mafic silicate absorption bands. The analysis of these increasingly complex mixtures centers on the effects of accessory phases on diagnostic mafic silicate spectral features for a number of reasons: (1) mafic silicates are both spectrally and compositionally dominant in a wide range of mafic and ultramafic assemblages such as basalts (Basaltic Volcanism Study Project, 1981), (2) the characteristics of mafic silicate absorption bands can be used to determine compositions and abundances and, (3) the other common accessory phases exhibit either weak or nonexistent diagnostic absorption features.

As there are three types of mafic silicates under discussion (OPX, CPX, OLV) the ensuing discussion will focus on how additional phases affect the spectral properties of the most studied phase, orthopyroxene, unless otherwise stated. This approach is further justified by the fact that absorption band strengths decrease in the sequence OPX-CPX-OLV. Olivine-orthopyroxene mixtures are the most intensively studied binary mafic silicate assemblage (Singer, 1981; Miyamoto *et al.*, 1983; Cloutis *et al.*, 1986). Spectral characteristics have been identified which are diagnostic of end member abundances, compositions and grain sizes (Cloutis *et al.*, 1986). Increasing olivine abundance shifts the band I minimum to longer wavelengths but does not affect the band II position (Table IV). The shift in band I position is not linear because olivine is a weaker absorber than pyroxene. The olivine absorption band is much wider than the pyroxene band I so that increasing olivine content shifts the interband peak to longer wavelengths. The lack of an olivine absorption band in the 2 $\mu$m region results in a decrease in the band II* /I* area ratio with increasing olivine content and the appearance of inflection points near 0.9 and 1.2 $\mu$m.

The presence of clinopyroxene in an assemblage is best recognized by the appearance of an absorption band in the ~2.1–2.4 $\mu$m region. Clinopyroxene absorption bands generally occur at longer wavelengths than orthopyroxene absorption bands, thus increasing clinopyroxene content shifts the band I and band II minima and the interband peak to longer wavelengths. Clinopyroxenes also have lower band II*/I* area ratios than orthopyroxenes, so as clinopyroxene content increases, band area decreases.

It has been amply illustrated that plagioclase is a weak absorber relative to mafic silicates (Adams, 1974; Nash and Conel, 1974; McFadden and Gaffey, 1978; Mustard *et al.*, 1986; Crown and Pieters, 1987). This leads to difficulties in spec-

TABLE IV

Effects of altering various mixture parameters on some spectral properties of orthopyroxenes

| | Band minimum position ($\mu$m) | | Interband peak Position ($\mu$m) | Band II*/I* Area ratio | Overall Reflectance |
|---|---|---|---|---|---|
| | I | II | | | |
| Add olivine | + | N.C. | + | − | +/− |
| Add clinopyroxene | + | + | + | − | +/− |
| Add plagioclase | +[3] | N.C. | + | +, −[4] | + |
| Add ilmenite/magnetite | N.C. | N.C. | N.C. | N.C.[5] | − |
| Reduce grain size[2] | N.C. | N.C. | N.C. | N.C. | + |

[1] For typical basaltic abundances of opaques.
[2] Assuming that absorption bands do not become saturated.
[3] Only at high abundances (>75 wt%).
[4] Increasing initially, decreasing when plagioclase abundance exceeds ~75%.
[5] May show a slight increase.
N.C. = no change.
+ = increase
− = decrease
+/− may increase or decrease depending on particular samples used.

trally identifying plagioclase in the ultraviolet, visible, and near-infrared spectral regions when mafic silicates are present. This is in spite of the fact that the plagioclase absorption band is not significantly overlapped by pyroxene bands. The changes in band area ratio (II*/I*) and interband peak position, which should be most sensitive to plagioclase abundance, have been examined for orthopyroxene + plagioclase mixtures. The band area ratio-plagioclase abundance relationship (Figure 18) illustrates the dominance of pyroxene; the band area ratio initially increases as plagioclase abundances increase but does not begin to decline to the (expected) plagioclase values until plagioclase abundance exceeds ~75%. If plagioclase and pyroxene were comparably absorbing, the trend should be roughly linear between the end members. It is apparent that only ~10% pyroxene mixed with plagioclase can be spectrally detected. The wavelength position of the plagioclase absorption band is comparable to the position of the orthopyroxene interband peak. Interband peak position determinations indicate that plagioclase abundances must be high ($\geq$80%) before peak positions are noticeably affected (Figure 17). At lower plagioclase abundances, its presence can be inferred by the flattening or skewing of the interband peak. Detection of moderate amounts of plagioclase ($\leq$ 50%) is difficult and better results may be obtained using other wavelength regions such as the mid- and far-infrared (Aronson *et al.*, 1967; Logan *et al.*, 1973; Walter *et al.*, 1987; Nash and Salisbury, 1990).

Opaque minerals influence reflectance spectra out of proportion to their abundances. The most important opaques for basaltic and many other M-UM assemblages are magnetite for terrestrial occurrences and ilmenite in lunar assemblages. These minerals do not possess well-defined absorption bands but tend to drastically reduce overall reflectance. Spectra L25, L3, and L12 illustrate the effect of increas-

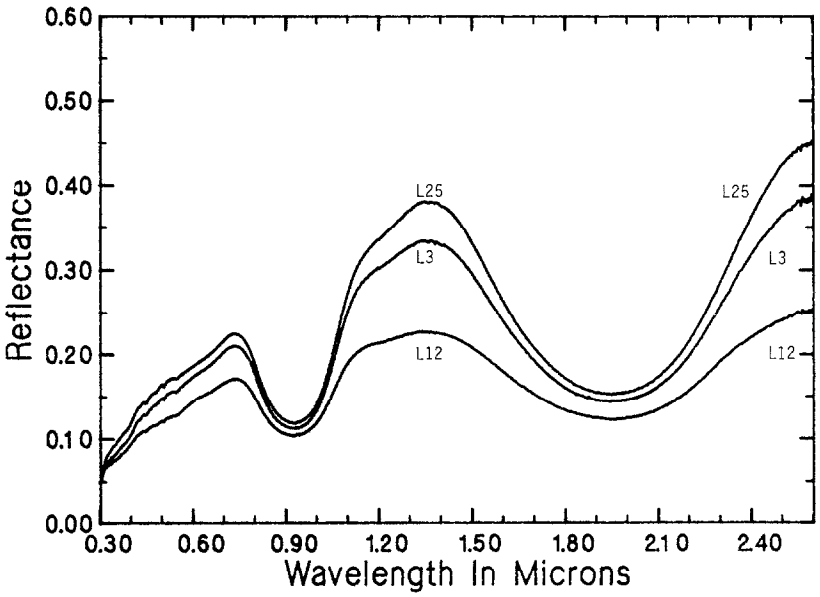


Fig. 24. Reflectance spectra of samples L25, L3 and L12 showing the effects of increasing ilmenite abundance on reflectance. End member abundances are listed in Table III. Spectra measured at RELAB ($i = 30°$, $e = 0°$).

ing ilmenite abundance on spectral reflectance (Figure 24). Ilmenite content increases from 0% (L25) to 6.7% (L3) to 25.3% (L12). The small difference in absolute reflectance between L25 and L3 could be enhanced by decreasing the grain size of the ilmenite. Even using this coarse-grained ilmenite (45–90 $\mu$m grain size), the reduction in overall reflectance with increasing ilmenite content is obvious. Band depths are reduced in the series L25–L3–L12 while band positions are relatively unchanged (Table II). The band area ratio shows an 8% increase from L25 to L12, a value much less than the variation between different orthopyroxenes (Cloutis *et al.*, 1986. 1990b). Consequently, mafic silicate compositions and end member abundances can be determined with a fair degree of accuracy using mafic silicate calibrations, in spite of the presence of opaques.

Grain size variations in mafic silicates are best determined using absolute reflectances or certain reflectance ratios (Cloutis *et al.*, 1986, 1990b). However, the addition of opaques reduces most reflectance ratios based on maxima and minima, as well as overall reflectance (Table IV). A decrease in reflectance ratios of mafic silicates usually implies a decrease in grain size which should be accompanied by an increase in overall reflectance. This difference can potentially be exploited to constrain opaque abundances and grain size ranges in a mixture. More laboratory work is being conducted in this area to examine the degree to which this effect is useful.

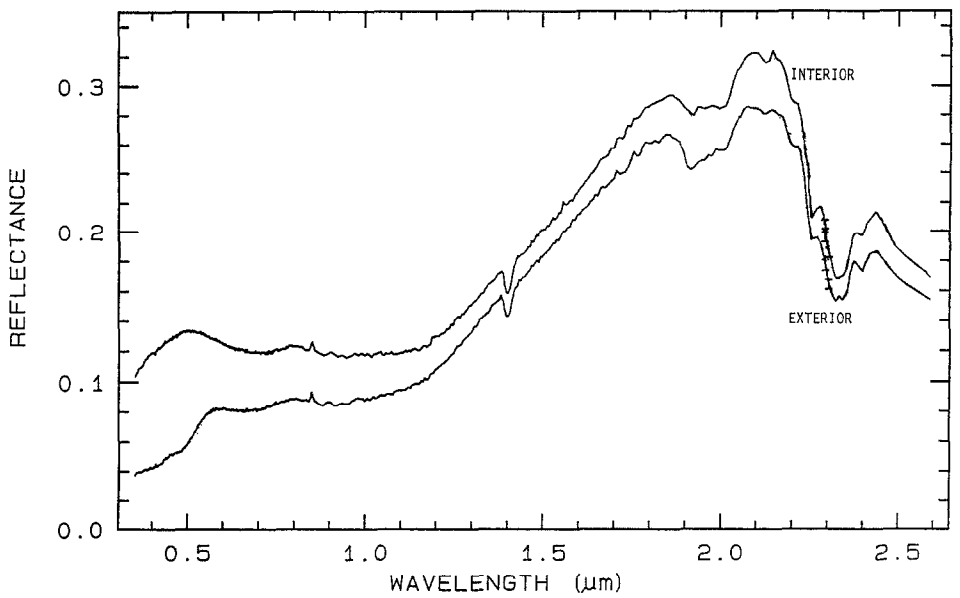


Fig. 25. Reflectance spectra of the weathered and unweathered surfaces of a basalt from northern Canada (measured at USGS).

## 9. Mafic and Ultramafic Rock Spectra

Reflectance spectra of various M-UM samples have been examined by a number of investigators but rarely in a systematic fashion; i.e. relating absorption bands to the compositions and abundances of various phases. Here, a survey of various M-UM spectral studies has been undertaken in order to assess the relative effects of the various components on reflectance spectra in light of the results presented for the constituent minerals and mixtures.

Mafic and ultramafic assemblages can largely be distinguished from acidic rocks because the different mineralogies result in differences in spectral properties. The presence of appreciable opaques in most mafic assemblages results in low overall reflectance, setting them apart from more acidic lithologies (Hunt *et al.*, 1974). Ultramafic sample spectra have overall reflectances intermediate between basic and acidic rocks but the presence of prominent ferrous iron absorption bands, particularly near 1 $\mu$m helps to distinguish them (Hunt *et al.*, 1974). This feature is particularly useful because it persists in samples showing moderate amounts of alteration (Hunt and Evarts, 1981).

The spectral interpretation of not only basalts, but most terrestrial rock spectra, is complicated by the presence of absorption bands due to weathering/alteration products. These features are most troublesome in the region of the pyroxene band II (>1.9 $\mu$m). Figure 25 shows the reflectance spectra of a lichen-free weathered and unweathered surface of a basalt from N. Canada. Visually, the weathered surface shows only weak evidence of weathering/alteration; a few restricted

patches of lichen and light grey areas superimposed on a uniform dark gray background. The interior surface of the sample is a saw cut face located ~1 cm below the weathered surface. There is no visible evidence of iron oxidation in terms of any rust-colored staining on either surface. In spite of the apparent unaltered appearance of the interior, both it and the exterior surface exhibit spectral features indicative of hydroxide-bearing phases. The absorption bands near 1.4, 1.9 and 2.3–2.4 $\mu$m are indicative of adsorbed and structural water and ligand-OH complexes, likely involving Mg (Hunt and Salisbury, 1970; Hunt *et al.*, 1974). This behavior is not atypical of naturally-occurring exposed rocks and illustrates the difficulties inherent in determining the nature of the mafic silicate phases present using procedures relying on band II, in particular. This problem would be minimized for freshly erupted/exposed samples.

The lichen-free weathered surface spectrum is similar in overall appearance to the unweathered surface but the ferrous iron absorption feature near 1 $\mu$m is only present in the unweathered spectrum. This indicates that while the weathered surface shows no evidence of iron staining, most of the ferrous iron in the optically sampled weathered surface has been converted to ferric iron (Sherman *et al.*, 1982; Morris *et al.*, 1985; Townsend, 1987). The presence of at least one mafic silicate can be deduced for the unweathered spectrum by the presence of the absorption band near 1 $\mu$m, attributable to ferrous iron. More detailed identification is not possible because any absorption feature near 2 $\mu$m is obscured by the ligand-OH absorption bands.

Many of the basalt spectra available in the literature are unaccompanied by the detailed compositional data required to relate specific spectral features to various physico-chemical properties. Adams (1968) presents three basalt spectra (Little Lake, Kilauea Iki, Boulder County) but no compositional information. However, all three spectra (<37 $\mu$m grain size) exhibit a well-defined absorption feature near 1 $\mu$m which is characteristic of mafic silicates and variable evidence for a 2 $\mu$m absorption feature. Other investigators have presented similar basalt spectra, all showing a ubiquitous absorption feature near 1 $\mu$m and a variable feature near 2 $\mu$m (Kuiper, 1969; Hunt *et al.*, 1974; Singer, 1980; Drury and Hunt, 1989). In other cases spectral features are absent because the scale of the plots is too large to permit easy identification of subtle absorption bands (Hunt *et al.*, 1974; Rowan *et al.*, 1977; Krohn, 1986). The strength, and hence detectability, of any mafic silicate absorption band is a function of opaque abundances, degree of crystallization and grain size. Ferrous iron absorption features are weakest in the least crystalline basaltic materials such as glasses (Adams, 1975; Cloutis *et al.*, 1990d). More detailed interpretations of basalt spectra can be made if accompanied by some compositional information. The spectrum of a nepheline basalt is very different from an olivine basalt, the latter showing clear spectral evidence for large amounts of olivine (Blake and Singer, 1984).

A large number of lunar basalt spectra have previously been measured. In all cases the dominant mafic silicate can be identified from the shape of the reflectance

spectrum (Adams and McCord, 1972; Adams, 1974; Charette and Adams, 1975; Pieters and Mustard, 1988). Most mare basalts which contain at least a few tens of percent of pyroxene exhibit reflectance spectra dominated by this phase (Adams and McCord, 1972; Adams, 1974). Charette and Adams (1975) have found that basalt classification can be accomplished using various spectral criteria. These criteria include the presence or absence of olivine absorption bands, band wavelength positions, strengths of plagioclase and ilmenite absorption bands, and slope changes in the visible region. Selected spectral criteria may also be useful for determining elemental abundances and some surface properties (Jaumann and Neukum, 1987; Jaumann *et al.*, 1988a,b). Once again, lunar basalt spectra are dominated by mafic silicate absorption bands and modified by plagioclase and opaques. The modification may be extreme in the case of samples exposed at the lunar surface for extended periods due to the formation of impact glasses and agglutinates (Adams and McCord, 1971a,b; Adams and Charette, 1975).

The II*/I* band area ratios for a large number of lunar and terrestrial basalt spectra have been measured. Lunar basalt band area ratios are sensitive to the presence of glass. Band area ratio decreases with increasing glass content (Adams and McCord, 1971b; Cloutis *et al.*, 1990d). For pure orthopyroxenes the ratio is ~1 and is <1 for clinopyroxenes. The lunar basalt spectra have band area ratios between 0.03 and 0.80 (Conel and Nash, 1970; Adams and McCord, 1971b; Adams, 1974; Adams and Charette, 1975; Charette and Adams, 1975; Pieters and Mustard, 1988). This wide range limits the interpretations which can be made for lunar basalts as a group using only band area ratios. Techniques for removing the spectral effects of glass are currently being examined (Cloutis *et al.*, 1990d). All that can be inferred for these spectra is that pristine orthopyroxene-rich (>80%) samples are absent in currently available lunar spectral data sets. The wavelength positions of lunar basalt spectra are more diagnostic than band areas but a detailed examination of the spectra is beyond the scope of this paper. See Charette and Adams (1975) and Cloutis *et al.* (1990d) for a more detailed examination of this issue.

Basaltic meteorite spectra are easily recognized by their shape and prominent absorption bands. Compositional variations can be determined from changes in absorption band shape and wavelength position (Gaffey, 1976; Morris, 1989). Such spectral variations have also been applied to determining compositional variations as a function of rotation for asteroid (4) Vesta (Gaffey, 1983).

The howardite and diogenite meteorites are orthopyroxene-rich groups with variable amounts of plagioclase (e.g. Dodd, 1981). Their reflectance spectra exhibit well-defined pyroxene absorption bands. The band II*/I* area ratio for various members of these groups have been plotted as a function of plagioclase content (Figure 18). The data generally follow the trend for the laboratory mixtures and some overlap between groups may be likely, even though none is shown for the small number of samples measured. Band area ratios seem to be very useful for identifying such meteorites and tentatively assigning them to a group. Howardites seem to exhibit higher band II*/I* area ratios ($\geq$1.2) than diogenites.

Spectral variations accompany changes in basalt particle sizes. Reflectance increases as particle size is reduced, as is normal for mafic silicates. However, overall spectral slope can also vary, becoming less red or even blue (reflectance generally decreasing with increasing wavelength) for whole rock spectra (Adams and Filice, 1967; Ross *et al.*, 1969; Singer and Blake, 1983; Pieters, 1989). The cause of this change in slope is not known but may be related to the change in natural grain size and redistribution of minerals which accompanies crushing (Singer and Blake, 1983). Similar changes are seen in reflectance spectra of carbonaceous chondrite meteorites (Johnson and Fanale, 1973).

Other mafic and ultramafic rock spectra show that mafic silicates are spectrally dominant phases where they are present in abundances $\geq$15%. Gabbro and diabase, composed predominantly of clinopyroxene and plagioclase, show well-defined pyroxene absorption bands, particularly near 1 $\mu$m. The presence of band II may be obscured by plagioclase which depresses the interband peak, effectively reducing the depth of band II (Conel and Nash, 1970; Nash and Conel, 1973; Hunt *et al.*, 1974; Adams and Charette, 1975). Increasing gabbro grain size results in a less red spectrum and reduced overall reflectance (Pieters and Hörz, 1985).

Lunar norites, composed predominantly of orthopyroxene and plagioclase, have reflectance spectra dominated by orthopyroxene and the presence of plagioclase manifesting itself as a prominent inflection on the long wavelength side of band I (Adams and Charette, 1975). Their band area ratios, 0.3–0.5 are lower than expected for a pure OPX-PLG assemblage (Figure 18), because of the presence of agglutinates and clear spectral evidence for clinopyroxenes in some cases, both of which serve to lower band area ratios. However, the interband peak positions lie near or above the upper range (1.4–1.5 $\mu$m) expected for mixtures containing 50–60% plagioclase (Adams and Charette, 1975). This shift to higher than expected wavelengths is probably due to the presence of agglutinates which shift the interband peak to longer wavelengths (Adams and McCord, 1971b; Cloutis *et al.*, 1990d).

More plagioclase-rich rocks, even those containing >60% plagioclase exhibit mafic silicate absorption bands as well as a moderately resolvable plagioclase absorption band near 1.2 $\mu$m (Conel and Nash, 1970; Blom *et al.*, 1980; Pieters, 1986). The most plagioclase-rich rocks, anorthosites, which contain only a few percent mafic silicates, may or may not display mafic silicate absorption bands (Adams and McCord, 1971b; Adams and Charette, 1975; Blom *et al.*, 1980; Pieters, 1986; Pieters and Mustard, 1988).

Olivine-rich rocks, such as dunites, have reflectance spectra showing the prominent olivine absorption band near 1 $\mu$m and a weak band near 2 $\mu$m if pyroxene abundance exceeds a few percent. Many of the spectra show evidence of aqueous alteration, complicating the determination of phase abundances using absorptions in the 2 $\mu$m region. The unaltered spectra have band II*/I* areas of $\sim$0 as expected. Band I minima are consistently between 1.05 $\mu$m and 1.08 $\mu$m, well within the olivine range, even when the samples are contaminated with minor

chromite or a few tens of percent of serpentine (Hunt *et al.*, 1974; Hunt and Wynn, 1979; Blom *et al.*, 1980; Hunt and Evarts, 1981).

Harzburgite and peridotite, composed predominantly of olivine and pyroxene, have reflectance spectra with absorption bands attributable to olivine and the particular pyroxene present (Hunt *et al.*, 1974; Hunt and Wynn, 1979; Blom *et al.*, 1980; Hunt and Evarts, 1981). Absorption bands may be only barely resolvable if the reflectance range of a spectrum is too large (Hunt and Wynn, 1979). The absence of detailed compositional information for most of these spectral samples precludes a more detailed analysis.

Pyroxenites are composed mostly of pyroxene and their reflectance spectra exhibit this dominance (Hunt *et al.*, 1974). Band positions can be used to quickly identify whether orthopyroxene or clinopyroxene predominates. Band area ratios are generally high ($>0.7$), as expected. Again, the quality of most of the available data precludes more detailed analysis based on band positions.

## 10. Conclusions

Recent advances in spectral characterization of the constituent minerals in mafic and ultramafic assemblages hold the promise for the development of improved spectral analysis techniques for deriving compositional information from their reflectance spectra. The major mafic silicate minerals, orthopyroxene, clinopyroxene, and olivine, are spectrally unique and distinguishable and their various spectral characteristics can be used to derive compositional information. For the purposes of spectral analysis, mafic and ultramafic rocks can be thought of as consisting of mafic silicate spectra modified by the presence of opaques, such as ilmenite and magnetite, and plagioclase feldspar.

Olivine reflectance spectra show a positive correlation between the wavelength position of the major absorption band near 1 $\mu$m and ferrous iron content. Orthopyroxenes show a similar correlation for both major absorption bands near 1 $\mu$m and 2 $\mu$m. Clinopyroxene absorption bands show a more complex relationship to ferrous iron content, exhibiting an initial decrease in band position with increasing ferrous iron content which gradually turns into an increase. Mafic silicate reflectance spectra show a decrease in overall reflectance and increases in band depths with increases in grain size.

The reflectance spectra of magnetite and ilmenite are generally flat and featureless. Their presence in a mafic silicate mixture results in a decrease in both band depths and overall reflectance. Key mafic silicate spectral parameters, such as band area ratios and band minima wavelength positions, are not appreciably affected by the presence of a few to a few tens of percent of these opaques, depending on particle size.

Correlations between spectral features and end member abundances and compositions are of variable quality for two component mafic silicate-bearing mixtures. Orthopyroxene-olivine mixture spectra can be analyzed in terms of band area

ratios and band positions to yield end member abundances and compositions, respectively. Clinopyroxene-olivine and orthopyroxene-clinopyroxene mixture spectra are less well constrained using spectral parameters, but broad limits can be placed on phase abundances and compositions. More sophisticated curve fitting techniques are required to yield more quantitative results (Sunshine *et al.*, 1990). Three-component mafic silicate mixtures (OPX + CPX + OLV) have not been intensively studied and only broad limits can be placed on phase abundances and compositions for assemblages containing subequal amounts of all three phases.

Opaque minerals such as magnetite and ilmenite are very effective at reducing overall reflectance and band depths of mafic silicates in small dispersed amounts. The reduction of both reflectance and band depths distinguishes opaques from increases in mafic silicate grain size. The presence of small amounts of opaques as found in basalts, does not appreciably affect key mafic silicate spectral parameters such as band positions and band area ratios.

Plagioclase feldspar displays only a single, weak, diagnostic absorption band near 1.25 $\mu$m over the wavelength region of interest (0.3–2.6 $\mu$m). Relative to mafic silicates, plagioclase has a much weaker absorption band and higher overall reflectance. Consequently, it has only a minor effect on mafic silicate spectra. Its presence is best detected by the distortion imparted to the pyroxene interband reflectance maximum near 1.4 $\mu$m, visibly distorting the peak when present at the few tens of percent level. Mafic silicate band area ratios and wavelength positions are relatively unaffected by plagioclase unless its abundance exceeds ~75%.

The reflectance spectra of mafic and ultramafic rocks, of which basalt is the most important, are dominated by the mafic silicates. Overall reflectance is generally low usually because of the presence of fine grained dispersed opaques. These spectra generally exhibit features characteristic of the spectrally dominant phase present and can be effectively interpreted using the various spectral deconvolution techniques available for simple mafic silicate assemblages, while making allowances for the presence of opaques and plagioclase.

## Acknowledgments

The authors wish to acknowledge, with thanks, the support provided through Grants-in-Aid of Research from Sigma Xi, The Scientific Research Society (to E.A.C.), the Geological Society of America (#3741–87, to E.A.C.) and NASA Planetary Geology and Geophysics Grant NAGW 642 (to M.J.G.). Thanks also to Drs. John Sampson-White and Pete Dunn of the Smithsonian Institution for providing a number of mineral samples, and to Dr. E. D. Ghent and John Macháček at the University of Calgary electron microprobe facility and Mr. Alex Stelmack at the University of Alberta for their help in characterizing the various mineral samples. Reflectance spectra were variously acquired at the University of Hawaii, at the NASA RELAB spectrometer facility at Brown University through the kind assistance of Dr. Carle Pieters and Stephen Pratt and at the U.S. Geologi-

cal Survey facility in Denver, Colorado through the cooperation of Dr. Roger Clark and Greg Swayze.

## References

Adams, J. B.: 1968, *Science* **159**, 1453–1455.
Adams, J. B.: 1974, *J. Geophys. Res.* **79**, 4829–4836.
Adams, J. B.: 1975, *Infrared and Raman Spectroscopy of Lunar and Terrestrial Minerals*, Academic Press, San Diego, pp. 91–116.
Adams, J. B. and Charette, M. P.: 1975, *Moon* **14**, 483–489.
Adams, J. B. and Filice, A. L.: 1967, *J. Geophys. Res.* **72**, 5705–5715.
Adams, J. B. and Goullaud, L. H.: 1978, *Proc. Lunar Planet. Sci. Conf.* **9th**, 2901–2909.
Adams, J. B. and McCord, T. B.: 1971a, *Science* **171**, 567–571.
Adams, J. B. and McCord, T. B.: 1971b, *Proc. Lunar Sci. Conf.* **2nd**, 2183–2195.
Adams, J. B. and McCord, T. B.: 1972, *Proc. Lunar Sci. Conf.* **3rd**, 3021–3034.
Adams, J. B., Hörz, F. and Gibbons, R.V.: 1979, *Lunar Planet. Sci. Conf.* **X**, 1–3.
Aoyama, T., Hiroi, T., Miyamoto, M. and Takeda, H.: 1987, *Lunar Planet. Sci.* **XVIII**, 27–28.
Aronson, J. R., Emslie, A. G., Allen, R. V. and McLinden, H. G.: 1967, *J. Geophys. Res.* **72**, 687–703.
Bancroft, G. M. and Burns, R. G.: 1967, *Am. Mineral.* **52**, 1278–1287.
Basaltic Volcanism Study Project: 1981, *Basaltic Volcanism on the Terrestrial Planets*, Pergamon, New York.
Blake, P. L. and Singer, R. B.: 1984, *Proc. Intl. Symp. on Remote Sensing of Environment, Third Thematic Conf. on Remote Sensing for Exploration Geology*, 785–795.
Blom, R. G., Abrams, M. J. and Adams, H. G.: 1980, *J. Geophys. Res.* **85**, 2638–2648.
Bruckenthal, E. A. and Pieters, C. M.: 1985, *Lunar Planet. Sci. Conf.* **XVI**, 96–97.
Burns, R. G.: 1970a, *Am. Mineral.* **55**, 1608–1632.
Burns, R. G.: 1970b, *Mineralogical Applications of Crystal Field Theory*, Cambridge University Press, New York.
Burns, R. G.: 1974, *Am. Mineral.* **59**, 625–629.
Burns, R. G., Huggins, F. E. and Abu-Eid, R. M.: 1972, *Moon* **4**, 93–102.
Charette, M. P. and Adams, J. B.: 1975, *Origins of Mare Basalts and Their Implications for Lunar Evolution*, Lunar Science Institute, Houston, pp. 25–28.
Clark, R. N.: 1980, *Publ. Astron. Soc. Pacific* **92**, 221–224.
Clark, R. N. and Roush, T. L.: 1984, *J. Geophys. Res.* **89**, 6329–6340.
Clark, S. P. Jr.: 1957, *Am. Mineral.* **42**, 732–742.
Cloutis, E. A.: 1985, *Interpretive Techniques for Reflectance Spectra of Mafic Silicates*, M.Sc. Thesis, University of Hawaii, Honolulu.
Cloutis, E. A., Gaffey, M. J., Jackowski, T. L. and Reed, K. L.: 1986, *J. Geophys. Res.* **91**, 11641–11653.
Cloutis, E. A., Gaffey, M. J., Smith, D. G. W. and Lambert, R. St J.: 1990a, *J. Geophys. Res.* **95**, 281–293.
Cloutis, E. A., Gaffey, M. J., Smith, D. G. W. and Lambert, R. St J.: 1990b, *J. Geophys. Res.* **95**, 8323–8338.
Cloutis, E. A., Gaffey, M. J., Smith, D. G. W. and Lambert, R. St J.: 1990c, *Icarus* **84**, 315–333.
Cloutis, E. A., Gaffey, M. J., Smith, D. G. W. and Lambert, R. St J.: 1990d, *Icarus* **86**, 383–401.
Conel, J. E. and Nash, D. B.: 1970, *Proc. Apollo 11 Lunar Sci. Conf.* pp. 2013–2023.
Crown, D. A. and Pieters, C. M.: 1987, *Icarus* **72**, 492–506.
Dodd, R. T.: 1981, *Meteorites, A Petrologic-Chemical Synthesis*, Cambridge University Press, New York.
Drury, S. A. and Hunt, G. A.: 1989, *Int. J. Remote Sensing* **10**, 475–497.
Evans, A. M.: 1980, *An Introduction to Ore Geology*, Blackwell Scientific Publications, Oxford.
Feierberg, M. A., Larson, H. P. and Chapman, C. R.: 1982, *Astrophys. J.* **257**, 361–372.
Gaffey, M. J.: 1976, *J. Geophys. Res.* **81**, 905–920.

Gaffey, M. J.: 1983, *Lunar Planet. Sci. Conf.* **XIV**, 231–232.
Gradie, J. and Veverka, J.: 1980, *Nature* **283**, 840–842.
Hapke, B.: 1981, *J. Geophys. Res.* **86**, 3039–3054.
Hazen, R. M., Bell, P. M., and Mao, H. K.: 1978, *Proc. Lunar Sci. Conf.* **9th**, pp. 2919–2934.
Huebner, J. S.: 1980, *Reviews in Mineralogy, Volume 7, Pyroxenes*, Mineralogical Society of America, Washington, D.C., 213–288.
Huguenin, R. L .: 1987, *Icarus* **70**, 162–188.
Hunt, G. R. and Evarts, R. C.: 1981, *Geophysics* **46**, 316–321.
Hunt, G. R. and Salisbury, J. W.: 1970, *Mod. Geol.* **1**, 283–300.
Hunt, G. R. and Wynn, J. C.: 1979, *Geophysics* **44**, 820–825.
Hunt, G. R., Salisbury, J. W. and Lenhoff, C. J.: 1971, *Mod. Geol.* **2**, 195–205.
Hunt, G. R., Salisbury, J. W. and Lenhoff, C. J.: 1973, *Mod. Geol.* **4**, 85–106.
Hunt, G. R., Salisbury, J. W. and Lenhoff, C. J.: 1974, *Mod. Geol.* **5**, 15–22.
Jaumann, R. and Neukum, G.: 1987, *Lunar Planet. Sci. Conf.* **XVII**, 460–461.
Jaumann, R., Kamp, L. and Neukum, G.: 1988a, *Lunar Planet. Sci. Conf.* **XIX**, 551–552.
Jaumann, R., Neukum, G. and Hawke, B. R.: 1988b, *Lunar Planet. Sci. Conf.* **XIX**, 553–554.
Johnson, T. V. and Fanale, F. P.: 1973, *J. Geophys. Res.* **78**, 8507–8518.
Johnson, P. E., Smith, M. O., Taylor-George, S. and Adams, J. B.: 1983, *J. Geophys. Res.* **88**, 3557–3561.
King, T. V. V. and Ridley, W. I.: 1987, *J. Geophys. Res.* **92**, 11457–11469.
Krohn, M. D.: 1986, *J. Geophys. Res.* **91**, 767–783.
Kuiper, G. P.: 1969, *Commun. Lunar Planet. Lab.* **6**, 229–250.
Logan, L. M., Hunt, G. R., Salisbury, J. W. and Balsamo, S. R.: 1973, *J. Geophys. Res.* **78**, 4983–5003.
Ma, M. S., Murali, A. V. and Schmitt, R. A.: 1977, *Earth Planet. Sci. Lett.* **35**, 331–346.
McCord, T. B. and Clark, R. N.: 1979, *J. Geophys. Res.* **84**, 7664–7668.
McFadden, L. A. and Gaffey, M. J.: 1978, *Meteoritics* **13**, 556–557.
McFadden, L. A., Gaffey, M. J., Takeda, H., Jackowski, T. L. and Reed, K. L.: 1982, *Proceedings of Seventh Symposium on Antarctic Meteorites, Mem. Natl. Inst. Polar Res. Spec. Issue Jpn* **25**, 188–206.
Miyamoto, M., Mito, A., Takano, Y. and Fujii, N.: 1981, *Proceedings of Sixth Symposium on Antarctic Meteorites, Mem. Natl. Inst. Polar Res. Spec. Issue Jpn* **20**, 345–361.
Miyamoto, M., Kinoshita, M., Takano, Y. and Takeda, H.: 1983, *Meteoritics* **18**, 356–357.
Morris, R. V.: 1985, *Lunar Planet. Sci. Conf.* **XVI**, 581–582.
Morris, R. V.: 1989, *Lunar Planet. Sci. Conf.* **XX**, 719–720.
Morris, R. V., Lauer, H. V. Jr., Lawson, C. A., Gibson, E. K. Jr., Nace, G. A. and Stewart, C.: 1985, *J. Geophys. Res.* **90**, 3126–3144.
Mustard, J. F. and Pieters, C. M.: 1989, *J. Geophys. Res.* **94**, 13619–13634.
Mustard, J. F., Pieters, C. M. and Pratt, S. F.: 1986, *Lunar Planet. Sci. Conf.* **XVII**, 593–594.
Nash, D. B. and Conel, J. E.: 1973, *Moon* **8**, 346–364.
Nash, D. B. and Conel, J. E.: 1974, *J. Geophys. Res.* **79**, 1615–1621.
Nash, D. B. and Salisbury, J. W.: 1990, *Lunar Planet. Sci. Conf.* **XXI**, 845–846.
Papike, J. J.: 1980, *Reviews in Mineralogy, Volume 7, Pyroxenes*, Mineralogical Society of America, Washington, D.C., pp. 495–525.
Pieters, C. M.: 1974, *Planets, Stars and Nebulae Studied with Photopolarimetry*, University of Arizona Press, Tucson, pp. 405–418.
Pieters, C. M.: 1983, *J. Geophys. Res.* **88**, 9534–9544.
Pieters, C. M.: 1986, *Rev. Geophysics* **24**, 557–578.
Pieters, C. M.: 1989, *Reports of Planetary Geology & Geophysics Program 1988*, NASA TM 4130, pp. 253–254.
Pieters, C. M. and Hörz, F.: 1985, *Lunar Planet. Sci. Conf.* **XVI**, 661–662.
Pieters, C. M. and Mustard, J. F.: 1988, *Rem. Sens. Environ.* **24**, 151–178.
Robinson, P.: 1980, *Reviews in Mineralogy, Volume 7, Pyroxenes*, Mineralogical Society of America, Washington, D.C., pp. 419–494.
Ross, H. P., Adler, J. E. M., and Hunt, G. R.: 1969, *Icarus* **11**, 46–54.

Rossman, G. R.: 1980, *Reviews in Mineralogy, Volume 7, Pyroxenes*, Mineralogical Society of America, Washington, D.C., pp. 93–116.
Roush, T. L.: 1984, *Effects of Temperature on Remotely Sensed Mafic Mineral Absorption Features*, M.Sc. Thesis, University of Hawaii, Honolulu.
Rowan, L. C., Goetz, A. F. H. and Ashley, R. P.: 1977, *Geophysics* **4**, 522–535.
Runciman, W. A., Sengupta, D. and Gourley, J. T.: 1974, *Am. Mineral.* **59**, 630–631.
Sherman, D. M., Burns, R. G. and Burns, V.M.: 1982, *J. Geophys. Res.* **87**, 10169–10180.
Singer, R. B.: 1980, *Lunar Planet. Sci. Conf.* **XI**, 1045–1047.
Singer, R. B.: 1981, *J. Geophys. Res.* **86**, 7967–7982.
Singer, R. B. and Blake, P. L.: 1983, *Lunar Planet. Sci. Conf.* **XIV**, 706–707.
Smith, J. V. and Steele, I. M.: 1976, *Am. Mineral.* **61**, 1059–1116.
Sunshine, J. M., Pieters, C. M. and Pratt, S. F.: 1990, *J. Geophys. Res.* **95**, 6955–6966.
Surkov, Y. A., Moskalyeva, L. P., Shcheglov, O. P., Kharyukova, V. P., Manvelyan, O. S., Kirichenko, V. S. and Dudin, A. D.: 1983, *Proc. Lunar Planet. Sci. Conf. 13th*, *J. Geophys. Res. Suppl.* **88**, A481–A493.
Surkov, Y. A., Moskalyeva, L. P., Kharyukova, V. P., Dudin, A. D., Smirnov, G. G. and Zaitseva, S. Y.: 1986, *Proc. Lunar Planet. Sci. Conf. 17th*, *J. Geophys. Res.* **91**, E215–E218.
Townsend, T. E.: 1987, *J. Geophys. Res.* **92**, 1441–1454.
Wagner, J. K., Hapke, B. W. and Wells, E. N.: 1987, *Icarus* **69**, 14–28.
Walter, L. S., Salisbury, J. W. and Vergo, N.: 1987, *Lunar Planet. Sci. Conf.* **XVIII**, 1052–1053.
Weidner, V. R. and Hsia, J. J.: 1981, *J. Opt. Soc. Amer.* **7**, 856–861.
White, W. B. and Keester, K. L.: 1966, *Am. Mineral.* **51**, 774–791.
Wood, C. A. and Ashwal, L. D.: 1981, *Proc. Lunar Planet. Sci. Conf. 12th*, 1359–1375.